FLUID PROPERTIES MEASUREMENTS USING PLANAR QUASI-SCHOLTE WAVEGUIDES

A Thesis Submitted to
The Graduate School of Engineering and Sciences of
Izmir Institute of Technology
in Partial Fulfillment of the Requirements for the Degree of

MASTER OF SCIENCE

in Mechanical Engineering

by
Okan BOSTAN

July 2017
İZMİR

We approve the thesis of **Okan BOSTAN**

Examining Committee Members:

Assist. Prof. Dr. Ünver ÖZKOL
Department of Mechanical Engineering, İzmir Institute of Technology

Assoc. Prof. Dr. H. Seçil ARTEM
Department of Mechanical Engineering, İzmir Institute of Technology

Assoc. Prof. Dr. Abdullah SEÇGİN
Department of Mechanical Engineering, Dokuz Eylül University

31 July 2017

Assist. Prof. Dr.Ünver ÖZKOL
Supervisor,
Department of Mechanical Engineering,
İzmir Institute of Technology

Dr.Onursal ÖNEN
Co-Advisor,
ASELSAN A.Ş

Prof. Dr. Metin TANOĞLU
Head of the Department of
Mechanical Engineering

Prof. Dr. Aysun SOFUOĞLU
Dean of the Graduate School
of Engineering and Sciences

ACKNOWLEDGMENTS

I would like to express my deepest gratitude to my advisor, Assistant Professor Ünver Özkol and my co-advisor Dr. Onursal Önen for their guidance, support, motivation, and encouragement during my thesis.

I am especially grateful to my laboratory friends, Yusuf Can UZ and Çağrı AKYOL for their support and assistance.

I would also like to thank Kutluhan GÜR, Ceren SEYRAN, Emre KOCAKU Cevahir KARAGÖZ and Rüzgar Efe TÜMER for their incredible support and help during this study.

Lastly, I offer sincere thanks to my family for their love, continuous counsel, and unlimited patience throughout my education.

ABSTRACT

FLUID PROPERTIES MEASUREMENTS USING PLANAR QUASI-SCHOLTE WAVEGUIDES

Interface acoustic waves can propagate in solid-solid and solid-liquid interfaces. They are perturbed by ambient conditions, interface materials and characteristics. The wave energy are shared between two interfacing media, with its distribution depending on these properties. In this study, it was aimed to make liquid characterization (density) using interface acoustic waves. The waves propagating between the plate and the liquid interface are kind of flexural waves and known as quasi-Scholte mode.

Firstly, the wave propagation for multilayered system is analytically modelled. A global matrix method is employed for obtaining the dispersion characteristics of the multilayer structure by considering the boundary conditions of the system.

In order to develop the dipstick sensor, liquid characterization is performed firstly by test cell method for longitudinal bulk velocity of the liquid with known density. Test cells with two different lengths were used for measurements. In this technique, transmitting and receiving transducers are placed on opposite sides of test cell. Based on the distance between transducers and time of flight, velocity of longitudinal bulk waves was calculated. Mixtures of ethanol-pure water were prepared at various ratios and measurements were taken at different temperatures.

Quasi-Scholte mode dipstick sensoring is employed by a simple measurement waveguide or dipstick inserted into the fluid to measure the velocity of the quasi-Scholte mode on a plate. This method, is based on mode conversions of waves. When the shear wave is excited on the aluminum plate, which is used as dipstick, Lamb waves occur at the solid-gas surface. The lamb waves are then converted into different modes in the solid-liquid interface. Leaky Rayleigh and Scholte propagating modes exist in immersed part as well. Quasi-Scholte wave propagate on the interface while the Leaky Rayleigh modes lose their energy. By means of dipstick method, alcohol water mixtures which is used in test cell method, were measured at room temperature.

The signals obtained as a result of the experiments were processed by the zero phase slope method. Time delay between reflected signals are found from phase slopes of the signals.

ÖZET

PLANAR QUASI-SCHOLTE DALGA KLAVUZLARI KULLANARAK SIVI ÖZELLİKLERİ ÖLÇÜMLERİ

Arayüz akustik dalgaları katı-katı ve katı-sıvı arayüzlerinde ilerleyen dalgalardır. Bu tip dalgalar, ortam koşulları, arayüzü oluşturan maddeler ve arayüz özelliklerinden etkilenirler. Dalgaların enerjileri, bu özelliklere bağlı olarak ortamlar arasında paylaşılır. Enerji dağılımı, dalgarın yayıldığı ortam hakkında bilgi edinmemize yardımcı olur. Bu çalışmada arayüz akustik dalgaları kullanılarak sıvı karakterizasyonu (yoğunluk) yapabilmek hedeflenmiştir. Sıvı ve katı bir plaka arayüzünde hareket eden dalga bir çeşit bükülme dalgasıdır ve yarı-Scholte olarak bilinir.

Ilk olarak, katmanlı yapılardaki dalga yayılımları analitik olarak modellenmiştir. Katmanlı yapılarda, dalga yayılımı karakterizasyonu için global matris metodu kullanılmıştır.

Daldırma çubuğu yöntemini gerçekleştirebilmek için, başlangıç olarak, yoğunluğu bilinen sıvıların boyuna yığın hızları test hücresi yöntemi kullanılarak bulunmuştur. Ölçümler için iki farklı uzunluktaki test hücreleri kullanıldı. Bu yöntemde yayıcı ve toplayıcı sensörler karşılıklı olarak test hücrelerine uygulanır. Mesafe farkı ve zaman ölçülerek dalgaların hızları ölçülür. Çeşitli oranlarda etanol-saf su karışımları hazırlanmış ve değişik sıcaklıklarda ölçümler yapılmıştır

Bir plakadaki yarı-Scholte modunun hızını ölçmek için sıvıya basit bir ölçüm çubuğu eklenebilir. Bu yöntemde, yarı-Scholte dalgasını kullanabilmek için, dalgaların mod değişimlerinden yararlanılmıştır. Daldırma çubuğu olarak kullanılan Al plakaya kesme dalgası uygulandığında, Lamb dalgaları oluşur. Lamb dalgaları katı-sıvı arayüzünde farklı dalga modlarına dönüşür. Sızıntılı-Rayleigh ve Scholte dalgaları katının sıvıya daldırılan kısmında oluşur. Bu modlardan yarı-Scholte modu sızıntılı-Rayleigh modunun aksine enerji kaybı olmaksızın arayüzde yayılır. Test hücresi metodunda kullanılan karışımlar daldırma çubuğu metodu ile oda sıcaklığında ölçülmüştür.

Deneysel olarak elde edilen dalgalar faz eğimi yöntemi kullanılarak işlenmiştir. Yansıyan dalgalar arasındaki zaman farkı faz eğimlerinin hesaplanmasıyla bulunmuştur.

TABLE OF CONTENTS

LIST OF FIGURES

CHAPTER 1

ULTRASONIC GUIDED WAVES

Ultrasonic waves have received great interest both in the industry and in research in recent decades. They are frequently used in non-destructive testing (NDT) and structural health monitoring (SHM) and in progress for applications in new fields. The most familiar method for ultrasonic non-destructive testing is through bulk waves which can be transducted into the target parts or materials easily by using piezoelectric transducers. Ultrasonic bulk waves travel in infinite media which have no boundaries. Bulk waves are categorized into Longitudinal and Shear waves that have a constant velocity with frequency. The reasons why bulk waves are preferred is their ease of use and not being complex for computation.

In some applications, use of bulk waves may become unfeasible, especially where access to target structure is limited or unsuitable for direct transduction, part to be inspected has large dimensions, and/or environmental and physical conditions are not suitable for transducers. For this reason, guided waves are used in these kinds of applications such as inspecting large structures, such as pipes, storage tanks, pressure vessels, guided waves are used. Unlike bulk waves, guided wave propagation mode relies on boundary conditions and these types of waves are result of the reflection, refraction, and mode conversation of longitudinal and shear waves at the interface of two materials. The main difference between guided waves and bulk waves is that, guided waves travel on the boundary (Rayleigh wave) or between the boundaries (Lamb wave) and use the structure as waveguide. Guided waves offer a wide variety of inspection possibilities for plates/shells, pipes, tubes, storage tanks, and many other structures. Many engineered structures can act as natural waveguides for guided wave applications [1].

In practice, bulk waves are employed to inspect very close area or directly beneath the applied area in the medium. But guided waves can be measured far away from the applied area. Comparison between guided wave and bulk wave is shown in Figure (1.1).

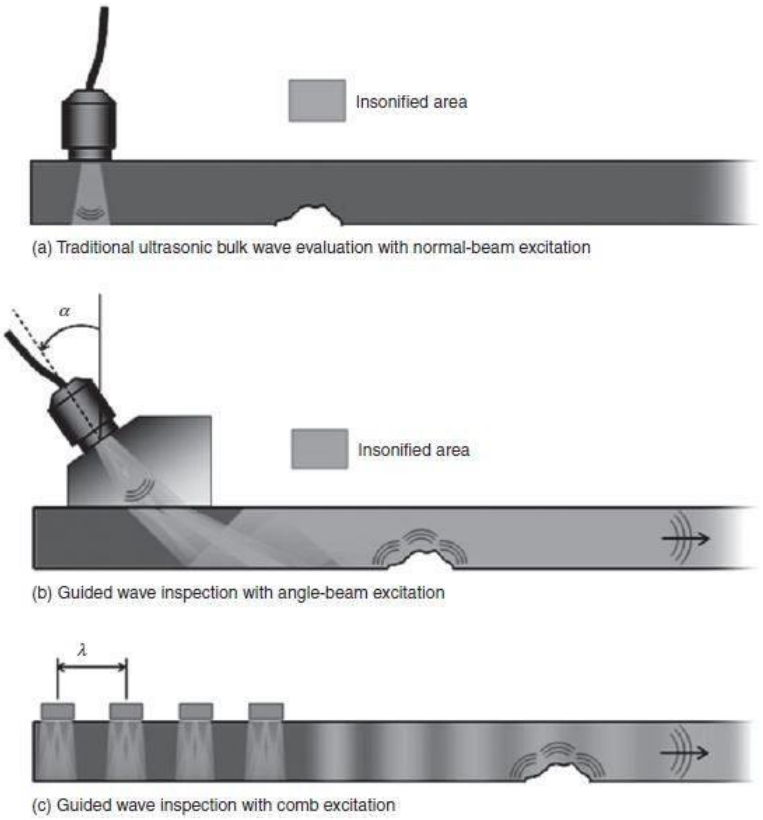

Figure 1.1. Bulk wave and guided wave methods in NDT [2]

Compared to other non-destructive methods, such as conventional bulk wave method [2], radiography [3], eddy current [4], guided wave analysis has lots of advantages. Rose presented in his book [1] some of these advantages and some are listed at below;

- It is possible to work on long distances by using single probe to take measurement.
- The measurements are more sensitive compared to traditional bulk wave ultrasonic methods.
- The ultrasonic guided wave techniques provide the inspection of hidden structures, structures under water, coated structures, structures under soil, and coated structures.
- Guided wave method is essentially inexpensive because of simplicity and rapidity. For example, there is no need to remove the coatings from a medium except probe position.

Bulk and guided waves are governed by same set of partial differential equations. However, the guided wave inspections require detailed analysis given the properties of these may change substantially with changing wavelength and frequency. Choice of the mode is important and understanding the dispersion characteristics of the propagating wave through-thickness is essential for choosing proper modes and frequencies for inspection.

Guided waves can propagate many different structures which are referred as a waveguide such as plate, pipe, and rods. In plate like structure, different wave modes can be occurred according to boundary conditions and thickness, wavelength relationship [5].

Guided wave method is widely used in food, chemistry industries and energy production. For example, measuring the properties of chemicals is impossible without opening its container. This process of opening container of hazardous chemical is usually very dangerous. But it is possible to measure a chemical's properties without opening the container using the special sensor. Likewise, in food industry, opening the containers of alcoholic beverages such as wine and whiskey lowers the quality of beverage, and makes it vulnerable to containment.

The aim of this thesis is to determine the fluid properties using planar guided interface waves. Scholte waves, which propagate at interfaces between solid-liquid medium is employed as the guided wave for this aim. The dispersion properties of these wave are the main reason of use. They can propagate for long distances without loss and they are highly affected by fluid properties. Transduction can be obtained firstly by generating Lamb waves in the wave guide, by use of piezoelectric transducers, which then propagate through a plate in air. As the wave reaches the solid liquid interface, this type of wave is turned into two types of wave: leaky Rayleigh wave and Scholte wave. Leaky Rayleigh wave is highly attenuated and loses its energy rapidly in a short distance in the liquid but Scholte wave are almost lossless and they propagate through the solid liquid interface. In the dipstick configuration, which is illustrated in Figure (1.2), the Scholte waves reflect back from the end of the plate with finite length and can be transducted back through the same mechanism and transducer.

Scholte wave energy is shared between solid and liquid according to their material properties.Scholte wave speed depends on frequency up to a certain value and this region are reffered as a **quasi-Scholte** (QS) mode. Above this value, wave becomes pure Scholte wave mode and speed of wave do not change with frequency. Thus, employing quasi-

Scholte mode propagating through the interface of solid and liquid, information on fluid properties can be obtained.

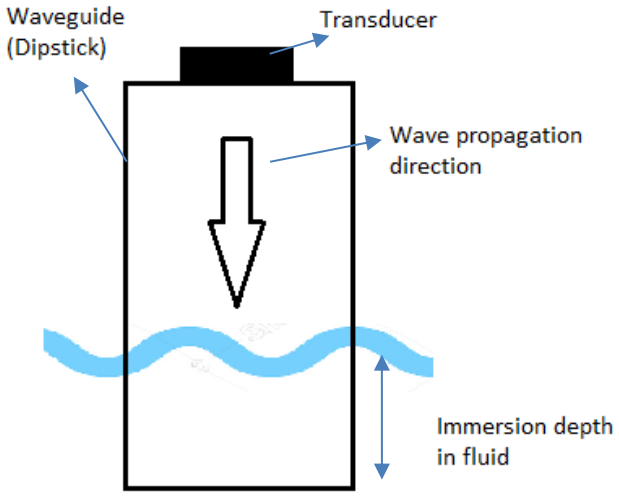

Figure 1.2. Dipstick configuration.

In this thesis, two types of test methods are used for investigating fluid properties which are test cell and dipstick method. Test cell method is the most conventional method for liquid characterization. This method is employed to measure bulk wave velocity of a wave propagating through a liquid in a container. This research intends to improve the understanding of guided wave propagation in liquid.

Outline of the thesis is as follows:

In Chapter 2, types of elastic waves are discussed and the advantages, disadvantages of using areas are compared. Dispersion and mode selection are briefly mentioned and test methods including generation and measurement of bulk and guided wave are explained. Finally, the historical development of the guided wave and the literature review are given in this chapter.

Chapter 3 contains the analytical and numerical methods used for wave propagation in Cartesian coordinate system. The model is established to evaluate dispersion curves for elastic and non-leaky layered or multi-layered systems.

Starting from Navier's equation of motion and Hook's Stress-Strain relation, stresses and displacements in a layer which is expressed by means of the amplitudes of

all of the bulk waves are obtained. Then, the global matrix is created to express the characteristic equation and associate all layers. A Numerical method is employed to solve the dispersion problem is also included.

Chapter 4 includes the experimental studies employed where determination of the fluid properties by using ultrasonic velocity in the alcohol-water mixture is used. Ethanol-water mixtures with varying concentrations were characterized using dipstick ultrasonic sensing method. These data are then compared with measurements taken with hydrometer. Samples are measured with both dipstick and test cell method. Then these measurement data are processed with signal processing and the sound propagation velocities in the mixture were determined. Uncertainties' of the method is presented at the end of the chapter.

In the final chapter, the overall studies are summarized.

CHAPTER 2

FUNDEMENTALS OF GUIDED WAVES

2.1. Acoustic Wave Types

2.1.1. Bulk Waves

Bulk waves travel in an infinite media, which means that the boundaries have no influence on the wave propagation. This type of waves can be categorized in two wave types which are longitudinal and shear waves.

In the longitudinal wave motion, the particles move parallel to the direction of wave propagation in which particles travel back and forth around their equilibrium pointes similar to simple harmonic motion. , Longitudinal waves can propagate through solid, liquid and gas media and also known as pressure waves or shortly P-waves.

Shear waves, also known as transverse waves or shortly as S-waves, are the types of waves in which the particle displacement is perpendicular to the direction to the wave propagation. The forces in S-waves create a shear effect in the medium, not alike the compression effect in P-waves. S-waves can propagate in solids, viscoelastic materials and highly viscous liquids.

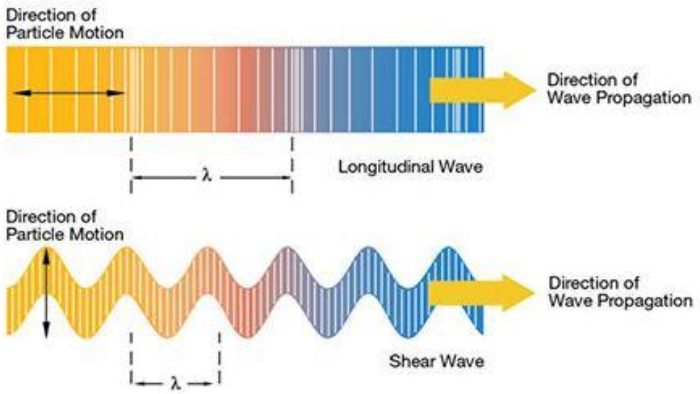

Figure 2.1. Longitudinal and shear wave propagation [6].

2.1.2. Surface Waves

2.1.2.1. Rayleigh Waves

Rayleigh waves are surface waves that propagate on elastic half space of semi-infinite solid [7]. Rayleigh waves occur by the combination of longitudinal and shear motion where the particles move in an elliptical path perpendicular to the surface. The particle movement on the surface are counter-clockwise. Deeper in the medium from surface, the shear effect of the wave decreases. The particle motion in the medium (about 1/5 of wavelength) becomes clockwise [8]. Figure (2.2) shows the decreasing amplitude of Rayleigh wave in the medium.

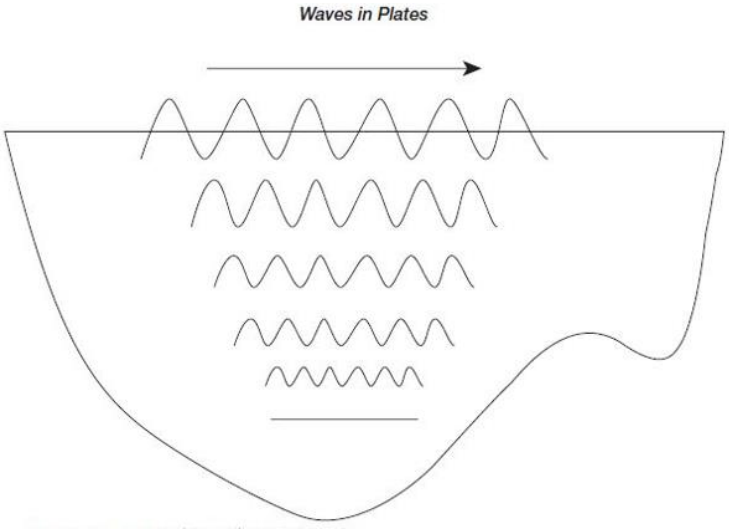

Figure 2.2 Rayleigh wave propagation [1].

2.1.2.2. Lamb Waves

Lamb waves are the waves that propagate in thin plates with traction free surfaces. Theory on Lamb waves also known as plate waves was firstly developed by Horace Lamb [9] on 1917. Reflections from boundaries and mode conversations of longitudinal and

shear wave lead to formation of the Lamb wave [10]. In Lamb waves, particles move perpendicular to the surfaces of the plate.

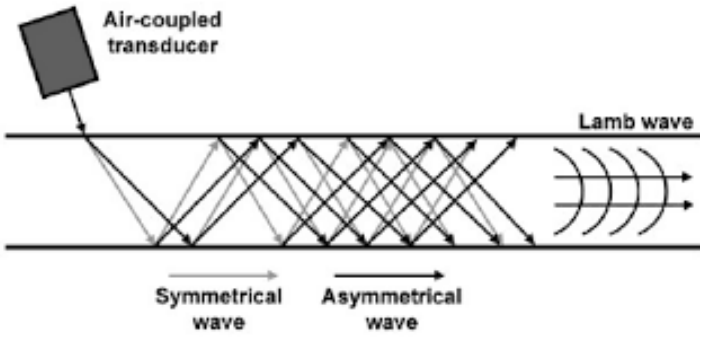

Figure 2.3. Lamb wave propagation [11].

In Lamb waves, there are infinite number of symmetric and anti-symmetric modes present, which have different characteristics with changing plate thickness and frequency. These modes also known as longitudinal and shear modes according to direction of average displacement of the plate thickness [12]. Figure (2.4) shows the schematic diagram of symmetric and anti-symmetric modes.

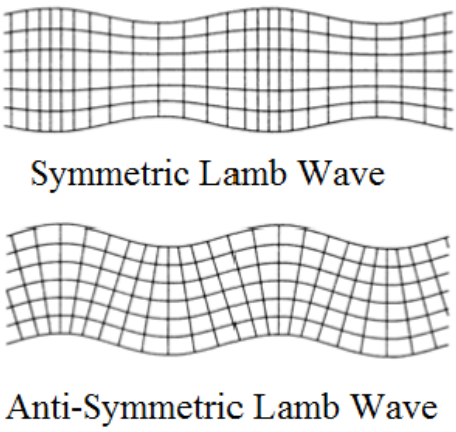

Figure 2.4. Diagram of symmetric and antisymmetric modes [13].

When the wavelength of the Rayleigh wave is smaller than the thickness of the plate, Rayleigh wave become Lamb wave. Generally, this conversation happens in low frequencies [14]. In high frequency, the wavelength may become shorter than the plate thickness, symmetric and anti-symmetric modes propagate with the same velocity of

Rayleigh waves in a half space. In this case, equal amplitudes of both modes give the single Rayleigh wave propagation.

2.1.3. Interface Waves

Interface waves are similar to the surface waves and this type of waves travel without energy loss at the solid-liquid and solid-solid interface. Significant features of the interface acoustic waves are as follows;

- Theoretically, there is no energy loss, for this reason, interface acoustic waves can travel for long distances.
- Unlike Lamb waves, there is single mode propagation in interface waves.
- The interface waves are dispersive (speed of the wave depends on frequency) up to a certain value for increasing thickness, frequency or thickness-frequency. As can be seen in Figure (2.5) that type of interface waves which is known as Scholte wave becomes non-dispersive approaching asymptotically to a limit value.

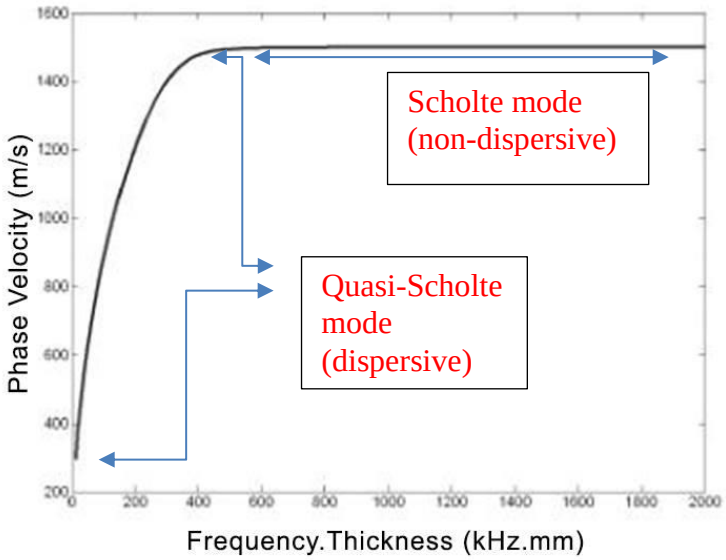

Figure 2.5. Scholte wave velocity against frequency, thickness multiplication [15].

- The velocity of the waves is always smaller than the all acoustic bulk velocities of the materials forming the interface. (At the silicon-water

interface, the sound velocity in the water is 1500 m/s, the speed of the interface wave is 1495m/s after the threshold value) [16].

- The energy of the waves is concentrated in the interface and shared between the materials forming the interface. Distribution of energy in between materials change according to the frequency thickness multiplication factor.

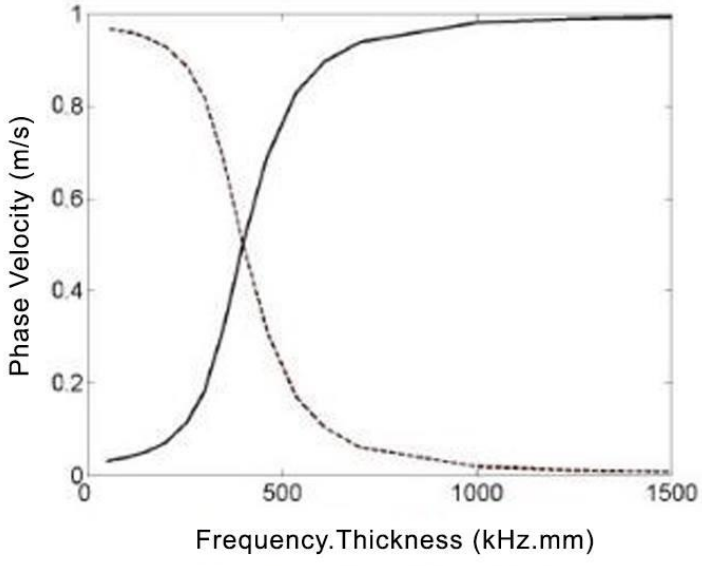

Figure 2.6. Sharing of interface wave energy between liquid (water) and plate (steel) according to the frequency-thickness multiplication [(—) flow of energy in liquid, (---) flow of energy in plate] [15].

2.1.3.1. Stoneley Waves

A seismologist Dr. Robert Stoneley (1924) discovered wave propagation between solid-solid interfaces [17]. This type of interface waves called Stoneley wave after his work. The Stoneley wave is an interface wave that typically propagates along a solid-solid interface. Generally, this type of waves is used for borehole sonic logging and vertical seismic profiling.

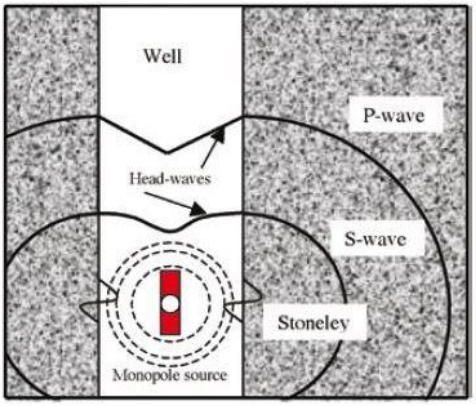

Figure 2.7. Stoneley wave propagation [18].

2.1.3.2. Scholte Waves

Scholte waves is an interface wave that propagate along solid-liquid interface that discovered by J.G. Scholte [19]. This type of waves, which are the main consideration of the thesis, move without energy loss in solid-liquid junction interface. The propagation characteristic of Scholte waves is directly related to longitudinal and shear horizontal wave speed of the interface forming materials [20].

In order to generate Scholte waves, the conversion of wave modes is commonly used [15, 22]. In this method, the interface waves are formed by the changing interface and boundary conditions from other acoustic wave modes. For example, surface acoustic waves are traveling in vacuum or gas interfaces of thick solids Figure (2.8. A), reflection between the solid-gas interface to the solid-liquid interface are shown in Figure (2.8.B), leaky Rayleigh waves Figure (2.8.C) and Scholte waves are also illustrated in Figure (2.8.D). Transformations of interface waves, surface acoustic waves and leaky Rayleigh waves are inevitable in interface changes. This method is the easiest and lowest cost method to generate and detect interface waves according to the following methods. However, the inability to control energy sharing in wave modes cannot be used efficiently due to energy loss in the leaky Rayleigh wave and wave modes.

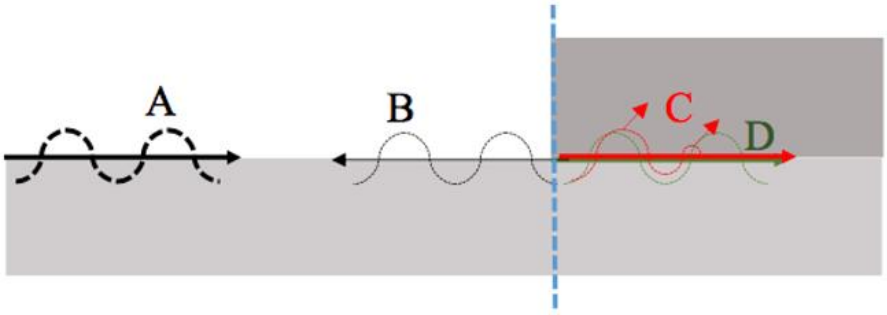

Figure 2.8. Reflection and transformation of acoustic surface wave on solid after entering solid-liquid interface, A: loading surface acoustic wave, B: acoustic wave reflecting from interface. C: leaky Rayleigh wave and D: Scholte wave.

As for the other generation techniques, laser applications and periodic material sequences are used for measuring acoustic interface waves. In laser ultrasonic methods, the wave transduction is utilized directly by fast lasers focused on the interface position [20, 21 22], by creating thermal stresses at the focal point with periodic radiation. While this method is efficient and selective to form interface waves, the high cost of lasers causes this method to be limited to laboratory applications. Interface waves can also be obtained by constructing phononic crystals from single-dimensional or two-dimensional array of materials and loading these structures with acoustic conversion devices [22, 25].

2.2. Fundamental Concepts

2.2.1. Phase and Group Velocity

Several frequency components make up an ultrasonic pulse. The shape of the pulse can be maintained if these frequency components have the same velocity along the propagation path. When they travel at different velocities, they will spread out from the source. In which case, wave velocity can be defined under two different concepts which are phase and group velocity.

Phase velocity is the velocity of a single phase of the wave propagating in space and can be define in terms frequency f and wavelengths λ :

$$c_p = \lambda \tag{2.1}$$

Or in terms of angular frequency ω and wavenumber k :

$$c_p = \frac{\omega}{k} \tag{2.2}$$

Group velocity, as the name implies, represents the velocity of the entire wave packet. This rate is determined by how fast the wave's energy is propagating down to the structure and this is always smaller than the bulk waves that occur in the same system [26]. The relationship between group and phase velocities is as follows:

$$c_g = \frac{d(kc_p)}{dk} = c_p + k\frac{dc_p}{dk} \tag{2.3}$$

Figure (2.10) shows the result of enveloped wave packet travels with group velocity c_g, and phase velocity of individual waves c_p.

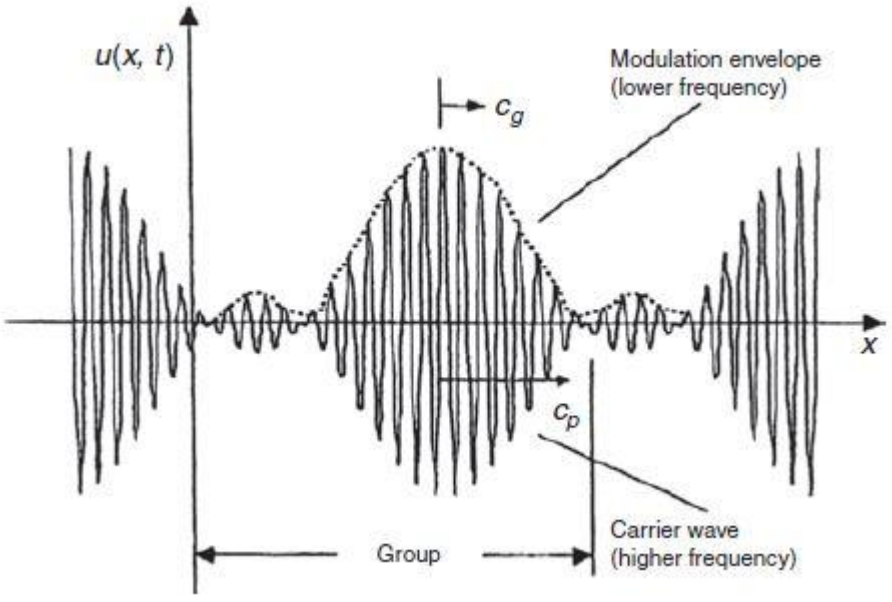

Figure 2.9. Phase and group velocity [1].

2.2.2. Dispersion

If the group and phase velocity varies with the frequency, this type of wave is called dispersive. Depending on to frequency, many modes can be present and propagate in a waveguide with each mode having their own phase and group velocities

Dispersion analysis of guided modes was firstly done by Lamb. According to Horace Lamb, analysis in infinite medium, only two type of wave modes (symmetric and asymmetric) travel at unique velocities, but plates support infinite number of Lamb wave modes. The propagation of Lamb waves in multi-layered structures cannot be solved analytically and requires a numerical approach. Many methods have been developed for such tasks. For instance, Rose has developed hybrid boundary element method (HBEM) [27]. Cawley used a traditional finite element method [28]. The strip element method for analysis was used by Achenbach (SEM) [29]. All those methods are applicable to almost any cross-section or structure configuration, but they are time consuming and stability of the solutions depends on frequency or the thickness (or product of these quantities).

Analytical methods are usually preferable for investigating guided wave problems since there is no numerical errors or instability problems and they are much faster. There are two main matrix methods for solving guided wave problems. They are Transfer Matrix Method (TMM) or Global Matrix Method (GMM). Transfer Matrix Method was introduced by Thomson in 1950 [30] and Haskell improved it [31]. In this method, stress and displacement of adjacent layers are related. The matrix for each layer is multiplied with the next layer to acquire the transfer matrix in multi-layer geometry. Then the boundary conditions are applied. The matrix remains the same size for wave propagation as the layer number increases. This makes Transfer Matrix Method applicable for multi-layer geometries. As an inconvenience though, matrix is unstable at high frequencies relative to layer thickness.

Global Matrix Method introduced by Knopoff in 1964 [32]. In this matrix, equations for wave propagation and boundary conditions are given in one single, and usually large matrix for multi layer problems. The matrix is solved as an eigenvalue problem as well as TMM. This method is more suitable, but the size of the matrix is bigger in multi-layered geometries and the solution is more time consuming. Lowe summarized two matrix methods in his paper [33].

In guided waves, dispersion results in the distortion of the shape of a multi frequency the wave packet propagating in long distances. This makes studying dispersion curves crucial for selecting wave mode and frequency.

Guided wave propagation depends on geometry. However, in plates, dispersion curves of phase velocity are plotted against frequency, time multiplication for normalizing with respect to the thickness. For example, phase velocity of 1mm thick plate at 0.5 MHz is the same as 0.5mm thick plate at 1MHz.

A typical phase velocity dispersion curve for a 1 mm thick steel plate is displayed in Figure (2.10). S and A represents the symmetric and anti-symmetric modes. Numbers shows harmonic order of symmetric and antisymmetric modes and SH waves as a function of the frequency-thickness product. Also, as it can be seen, when the frequency increases, more mode solutions exist in plate with wavelength getting shorter.

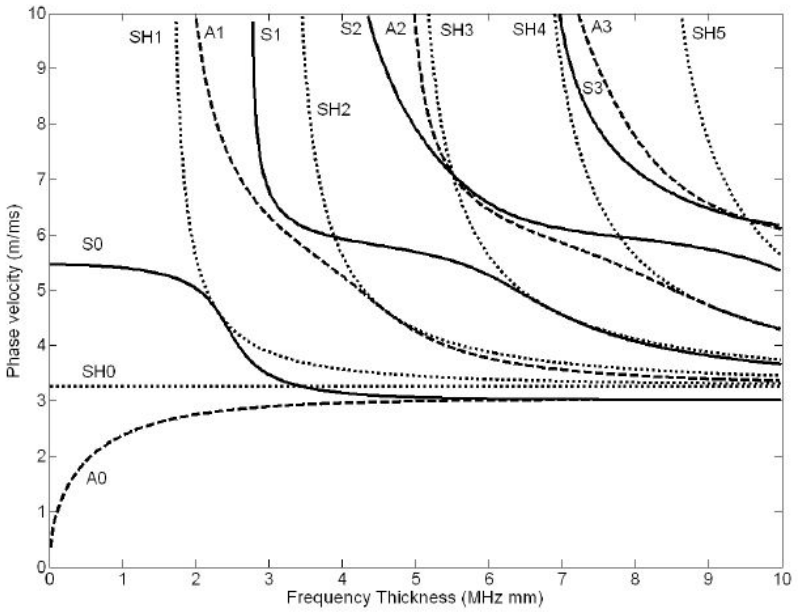

Figure 2.10. Phase velocity dispersion curves of a 1mm steel plate: Longitudinal modes (—), Flexural modes (---) and Torsional modes (· · ·) [only order 0 and order 1 modes are shown] [34].

2.3. Mode Shapes

The mode shape of a propagating mode can be represented in terms of displacement, stress, or other related property variations across the cross section of the waveguide and surrounding media. Usually mode shapes are displayed the position

against the amplitude of displacement or stress component of the mode. The mode shapes are of arbitrary absolute amplitude but show the correct relative amplitude compared to another displacement or stress component.

In the limit of low frequency and thickness products, the displacement mode shape of each of the fundamental mode is uniform across the section and in the direction of polarization. At higher frequency and thickness products, the mode shape will start to vary across the thickness of the plate.

The dispersive or (quasi-) Scholte waves, which are main subject of this thesis are flexural waves. These waves mainly cause out-of-plane displacements in the plates. The Figure (2.11) is taken from the work of Cegla [34] showing the mode shapes of quasi-Scholte wave at different frequencies which propagates interface of 1mm thick steel plate and water for 0.1 and 0.5 MHz.

At low frequencies, as can be seen in Figure (2.11a), out-of-plane displacement is almost constant throughout the thickness of the plate, and strain energy density also showing that most of the proragating wave energy travels on the plate. At higher frequency as shown in Figure (2.11b) most of the energy of Scholte wave is concentrated in the fluid domain. As a resulting of that, in order to make characterization of the interface materials can be investigated in a very specific frequency range where the energy distribution are included with both materials. This relation also mentioned in previous section in Figure (2.6). For this reason, in order to determine these frequency range, mode shape of the Scholte waves is used in specific studies.

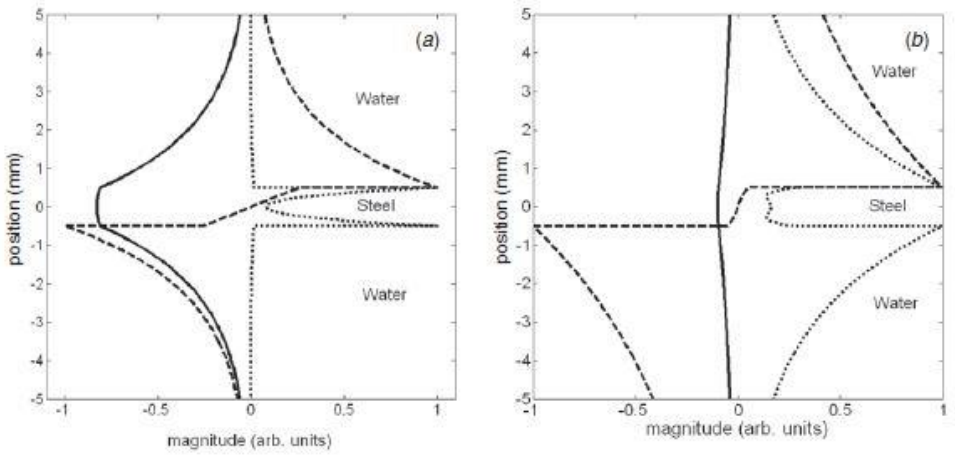

Figure 2.11. Mode shapes of the quasi-Scholte mode at water and 1mm thick steel plate: (a) 0.1 MHz mm, (b) 0.5 MHz mm ,(c) 2 MHz mm (in plate only) ((——) out-of-plane displacement, (– – –) in plane displacement and (…) strain energy density) [34]

2.4. Ultrasonic Sensing

Ultrasound waves are high frequency waves that can be generated by several methods such as electrostatic, electrodynamic, magnetostrictive and laser techniques [2]. Beside these methods, most preferred ultrasound generators are based on the piezoelectric effect due to its simple construction and operation, which makes them suitable for various applications.

Piezoelectric ultrasound generators are, also known as transducers, consists of a layer of piezoelectric material and thin metal electrodes in contact with each other. If an electrical voltage difference is applied to these materials, the thickness of the piezoelectric material will change depending on electrical field, thus transformations of electrical energy into mechanical energy is achieved. Also, if a piezo-electric material is deformed mechanically, electrical energy is produced on its surface. This effect firstly discovered by Curie in 1880 [35]. The active elements that transforms the energy are usually crystals or ceramics [36]. Each transducer has a natural frequency dependent on thickness of piezo-electric material. [37]

There are varieties of piezo-electric transducers according to applications such as contact and immersion types. Immersion type transducers are used in liquid environment. Specially designed angle beam are used for generating shear waves. In angle beam transducers, surface of probe fixed on a reflector with a certain angle. Required mode of wave is obtained as a result of this incidence angle. The incidence, reflection and transmission can be calculated with Snell's Law [38]. Alternatively, normal incidence transducers are used for generating shear waves without using angle beam wedges.

The basic principle of ultrasonic sensing of materials is propagation and reflection of sound waves. When the generated sound wave by transducers applied in medium, wave energy transmitted by colliding particles. When the sound wave reached another medium, it is reflected back to the source, or transmitted to the neighboring media. Free ends can also reflect the wave. When there is discontinuity in medium such as a cavity, crack etc., and transmitted wave may reflect from the discontinuity and arrive back to the transducer earlier. There are two types of test methods known as pulse-echo and through transmission which utilized the echo of defect for material testing. In pulse-echo testing, a transducer performs both the sending and receiving of the ultrasonic pulse. In through transmission testing, two probes are used as transmitter and receiver and they are located

at opposite sides of the material. These methods also used for determining the bulk properties of liquids and known as test cell method. [39]

Test cell method is the most conventional method for liquid characterization. Especially when testing attenuative materials, the gap between the transducers must be adjusted carefully. The disadvantage of test cell method is to have too much sound wave reflection which effects measurements in an unfavorable way and creates noise. For this reason, the surfaces of test cells must be designed according to these reflections. Also, transducers should be in good contact with the cell or liquid in this system. Major problems of such systems are that, the transducers can be depolarized in measurements at high temperatures (250 °C) for high temperature applications or can be damaged under high heat radiation [34].

Studies for manufacturing transducers that are durable to these effects are on progress, but not preferred due to their high cost. Systems that utilize waveguides, through which the waves can safely propagate, by separating the transducer and target such as dipstick method, are much cheaper and preferred. Cegla [34] applied this method to fluid sensing and interface waves are used to characterize materials

In the dipstick method, a wave is emitted to the plate, which is submerged to the fluid that needs to be characterized. Scholte waves can be identified as a wave between liquid and solid boundaries. Energy of Scholte wave propagates to the liquid from the plate. This wave is sensitive to the properties of liquids. Wave energy concentrated around the perimeter of plate [39].

2.4.1. Ultrasonic Sensing Using Guided and Interface Waves

Ultrasonic sensing has been used number of years in ultrasonic applications of non-destructive testing (NDT) and structural health monitoring (SHM) of engineering structures such as railways, pipes and plates. Guided waves are capable of detect defects and discontinuities of large areas, multilayered, underwater structure or coatings. For example, Lamb wave propagation is affected by cracks and other defects in a structure. For this reason, the generation and sensing of Lamb waves in a structure can give information on structural damage. On the other hand, Rayleigh waves travel along the surface and their energy decreases with the depth and this decrease rate depends on wavelength. For this reason, Rayleigh waves are generally used for detecting surface

defect. Other examples of guided wave include Stoneley and Scholte wave. These types of waves are not commonly used for damage detection because they occur at the interface of solid-solid and solid-liquid [40]. Some studies on the usage of these commonly used waves in industrial applications are explained below.

Firstly, Cawley et al. [41] realized the availability of Lamb waves for the inspection of large areas due to their capabilities of propagating long distances. They discuss the single mode and frequency excitation in a near non-dispersive region according to application. Lowe et al. [42] worked on optimum mode selection according to defect size, and strength of reflection.

Zhu et al. were presented an experimental study and they have focused on detection of hidden corrosion by using ultrasonic guided waves [43]. Chang et al. worked on mechanism of reflection and transmission structure when Lamb waves pass through crack or material defact. Using this mechanism, material loss, cracks or other flaws can be identified, whether they exist or not [44]. Wang et al. presented a method for detecting the damage on the concrete and composite materials. Their method is based on time of flight of the scattered reflection from the damage [45]. Yuan et al. proposed a technique that is based on energy propagation of Lamb waves to detect the damage location in an isotropic plate [46].

In 1967, Viktorov presented a study about basic properties and relation between Rayleigh and Lamb wave [47]. In his work, scattering surface wave from defect was investigated experimentally by using comb and wedge transducers. According to his work, defect depth can be defined by using oscillation period in the frequency domain. Hall published another work for detect the defect depth by using pulse-echo method during fatigue testing on rails [48]. Analytical formulations of Rayleigh wave which reflects and transmits the wave by surface breaking crack for normal and oblique incidence, are presented by Achenbach et al. [49] and proved experimentally by Adler et al [50].

Tubing inspection with ultrasonic guided waves was first introduced by Rose et al. [51]. In this work, theoretical background of guided waves in tubes is investigated and Li and Rose presented the phase array focusing technique for longitudinal guided wave propagation in cylindrical shells [52]. Thompson et al used Lamb waves for steel plate and pipe inspections for studying circumferential waves [53]. Coating disband detection methods with guided waves were developed by Van Velsor et al. [54].

Chimenati used leaky-lamb waves in fluid-coupled composite laminates for detecting and imaging bond flaws [55]. A more effective ultrasonic guided wave inspection method for a titanium patch bonded to an aluminum aircraft body was introduced by Puthillath and Rose et al [56].

Guided wave mode and frequency selection was studied by Gao et al. for tomography to scanning aircrafts [57]. Van Velsor et al. 2007 studied detection of pipe defects with guided wave tomography [58].

2.4.2. Fluid Characterization Using Interface Waves

Developing guided wave technology is emerging as a fluid characterization tool by using ultrasonic waves. Complex fluids are used in many industries and products such as food, painting, and oil. For the best quality, ingredient of these fluids and their mixing ratios are very important. Particle size, density, contents of fluid, phase transition and many properties could be measured by using ultrasonic waves.

Conventional ultrasonic measurements are based on determining the sound velocity in medium. The time of flight of a distance between a receiver and a transmitter is used for this purpose. In every medium, propagation velocity of sound depends on bulk modulus and the density of medium, and also these may change with respect to changing environmental conditions such as temperature. If bulk modulus and sound speed are known, density can be found by computation.

Another approach for determination of density presented by Graff [59]. Their measurement method based on reflected wave amplitude from interface of known and unknown materials. Reflection coefficient depends on acoustic impedance of materials, which may be defined as multiplication of wave velocity by the density.

According to these methods, some properties must be known to measure density of material. As an alternative, the dipstick method was presented by Cegla [39]. Cegla worked on fluid characterization using interface waves. In this study, two different methods were used for characterization of the fluids. In order to obtain the results, Quasi-scholte wave was applied in range of different temperatures. The sample sizes are approximately 25 ml for the conventional test cell and 200 ml for the quasi-Scholte mode setup. The prepared samples were monitored with the aid of thermocouple in a liquid environment set at 25 °C. Some of the properties of the setup are 0.105mm in thickness,

96mm in width, 135mm in length and the material used is stainless steel. In addition to these properties, the quasi-Scholte mode setup has 5MHz shear transducer (Panametrics Inc.). This shear transducer installed to its end at the center of the width. Hanning windowed with 5 cycle signal was used to excite the A0 mode.

Firstly, the ultrasonic test cell method was used. In this method, the fluid was placed in a cell and two probes are placed opposing each other. One of these probes is transmitter, the other one works as receiver as shown in Figure (2.12)

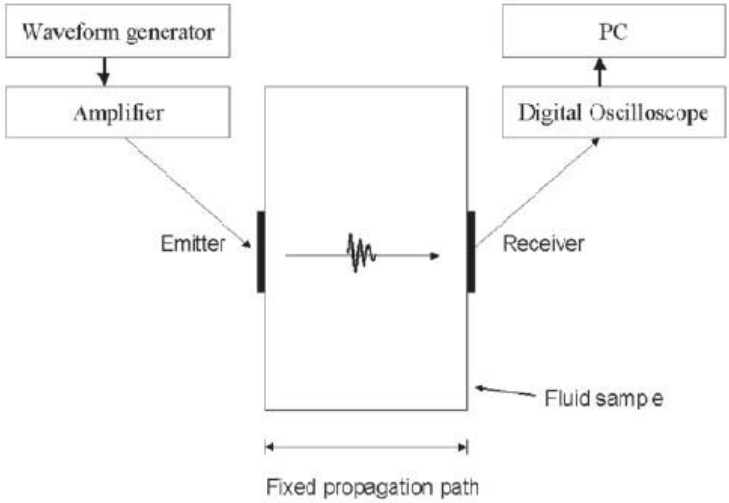

Figure 2.12. Ultrasonic test cell method [2].

According to second method which is the dipstick method, group velocity and attenuation of the fluid are measured by using quasi-Scholte mode in a plate dipped in the fluid. Shear transducer is fixed perpendicularly on top of the plate. The transducer fixed on the plate is used both as a transmitter and a receiver. A0 flexural wave is transmitted throughout the plate. When the wave hits the liquid, most of its energy is attenuated but only the quasi-Scholte wave remains to propagate in the fluid. The wave that transmitted in the fluid is received by the end of the plate, and then converted to electrical signal by the transducer through inverse piezoelectric effect. Figure (2.13) shows the experimental setup of the dipstick method.

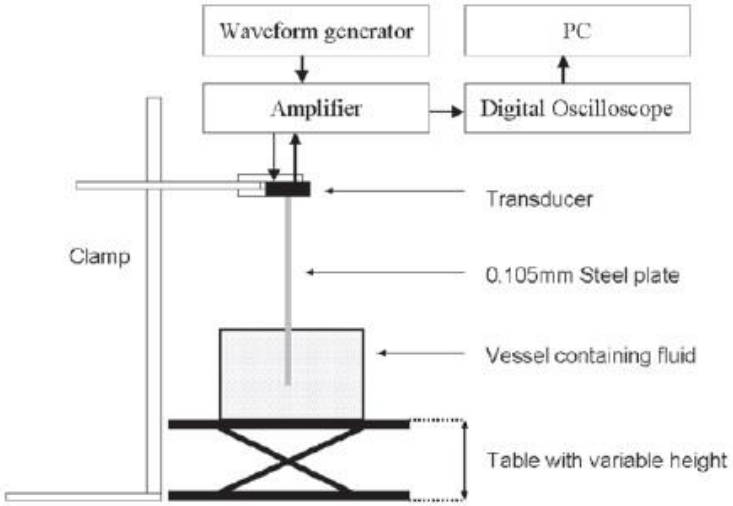

Figure 2.13. Dipstick sensor method [39].

Quasi-Scholte wave contains information about bulk properties of the liquid. In calculating the group velocity; x_2 and x_1 which are different immersion depths, time delay between two wave packages and c_gA0 (group velocity of A0 plate mode) were used. In order to find the time difference, Fourier transform and cross correlation method were used in the center of frequency at two different immersion depths.

The density and viscosity of a glycerol (98%–99% pure) sample was measured at 25°C. Secondly, these methods were used to determine honey properties. Further measurements were examined on water and suspension which is silicon dioxide. It has 1% volume fraction and average diameter is 1-5mm in water. The particles were stirred and immersed ultrasonic bath to measure the properties. Using test cell and dipstick methods measured viscosities of glycerol agree within 4%. The results for measured viscosity of honey is well within 3,5%. This means that the method can also retrieve data from very viscous fluids.

Velocity results were obtained by %5 error. Error in group velocity measurements was determined to be inaccuracy of positioning the plate. Quasi-scholte mode measurements at attenuation are sufficient to determine viscosity of the Newtonian fluids. However, Quasi-scholte mode could not be used to determine viscosity in non-Newtonian fluids alone. In ultrasonic test cell method, there are some deficiencies such as measurement of highly attenuating fluids or measurements in systems that has moving medium.

Another study for determination of fluid properties using interface wave was presented by A.E. Takiy et al. [60]. This work uses an analytical technique for modeling the propagation of interface waves in a viscous fluid on partially submerged plates. Modeling was done based on Navier-Stokes equation for viscous fluid. Modeling of multilayered media which consists of fluid-plate-fluid was completed using global matrix method. Phase velocity and attenuation curves were examined as a function of frequency and theoretical calculations were used. Applicability of using the quasi-Scholte mode in fluid analysis was confirmed via an experimental method. In these experiments, phase velocity values were measured for quasi-Scholte mode in distilled water and different ethanol-water concentrations (7.57%, 16.14%, 23.85%, 33.64%, 42.30%, 52.28%, 74.30% and 97.39%). As a result of this study, some waveforms were obtained and the velocities which are function of frequency were calculated. In experiments 0.1 mm thick stainless steel and 3 MHz transducers was used. 9 ml capacity container with the liquid sample was placed in a temperature controlled water bath and maintained at a constant temperature of 20 °C.

In the signal processing, sliding Gaussian window was used for smoothing the signal and removing undesired echoes. To analyze the signal, FFT and phase curves was used to calculate the phase velocity curves. Experimental and theoretical results are shown graphically.

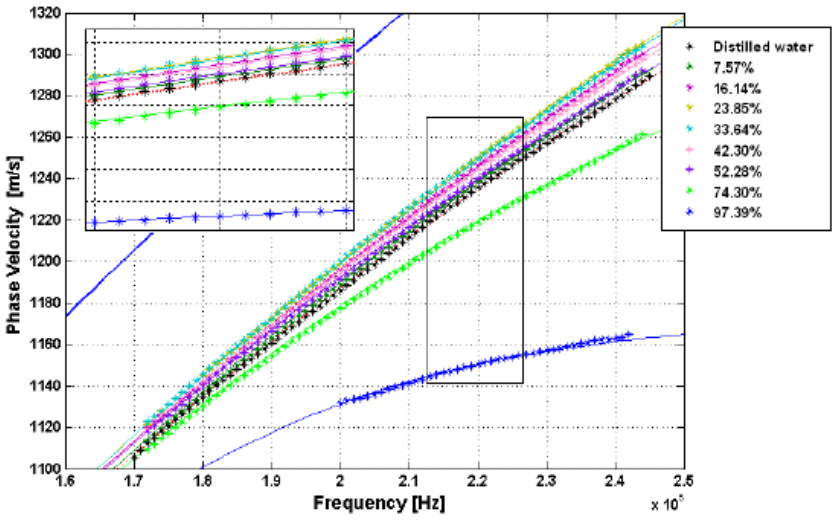

Figure 2.14. Theoretical and experimental phase velocity curves of various mixture [60].

Another work based on viscous fluid characterization by using a Lamb wave sensor was worked by Nicholas Wilkie-Chancellier [61]. In this study, a new type of sensor fixed on a stainless-steel plate in contact with a viscous fluid is employed. Piezo-electrical material is placed on an angled Plexiglas part. Lamb waves are used and reflected waves at boundy interface are measured for characterization. The progression modes of the loaded plate are investigated. The viscosity of the material contacting the metal was found by monitoring the mechanical impedance. Wave propagating through Plexiglas to the plate, create Lamb wave. A1 Lamb wave mode was used to detect the fluid parameters.

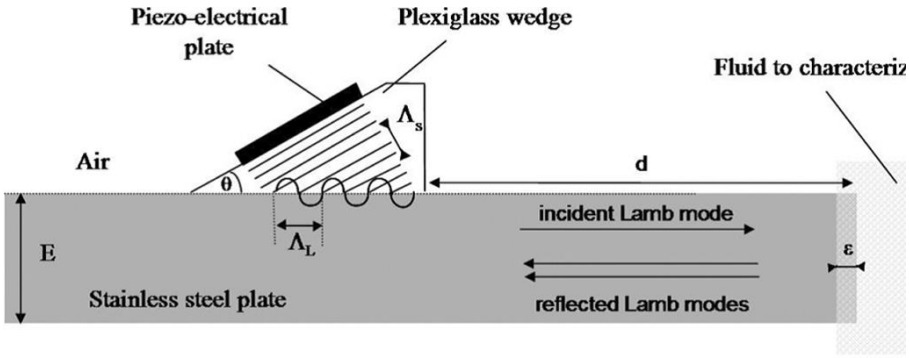

Figure 2.15. Description of Lamb wave sensor [61].

The transducer is a piezoelectric plate (25x35mm) with a 1,5 mm thickness and a Plexiglas wedge to have a θ angle with the plate. The wedge is at a d=10mm distance from the plate end. This wedge transducer is a chosen to generate a linear Lamb wave front (25 mm wide) at the resonant frequency 1.25 MHz. Two different asymmetric (A0 and A1) and one symmetric mode (S0) can be used for this frequency-thickness product. There is no change of symmetry modes were observed at the reflection, in addition with the normal free edge. The wedge angle is chosen to be 24 degrees to generate A1 Lamb mode according to the Plexiglas properties, because A1 Lamb mode is more sensitive to the conversion rate.

A burst signal of twenty periods is applied to the transducer to generate A1 Lamb wave. A laser vibrometer coupling with a micro-positioning system was used to measure displacements along the propagation.

It is concluded that A1 Lamb waves can be used for characterization of fluids. The experimental results show, this method can measure the viscosity for weak viscous fluids. The results also show that the extracted dynamic viscosity for Newtonian fluids

can be measured by a small error margin. This concludes that presented method can be a new method for fluid characterization.

A case study of guided waves in a steel plate one side immersed in water is published by Lingyu Yu [62]. Using guided waves for evaluating plate surface condition change due to the presence of water is discussed. These leaky waves have different properties such as mode shape, attenuation and wave speed compared to the guided waves in free plates.

A scanning laser vibrometer is used for wave actuator and a hybrid sensing system using PZT for acquiring data and 2D Fourier transform for analyzing the data.

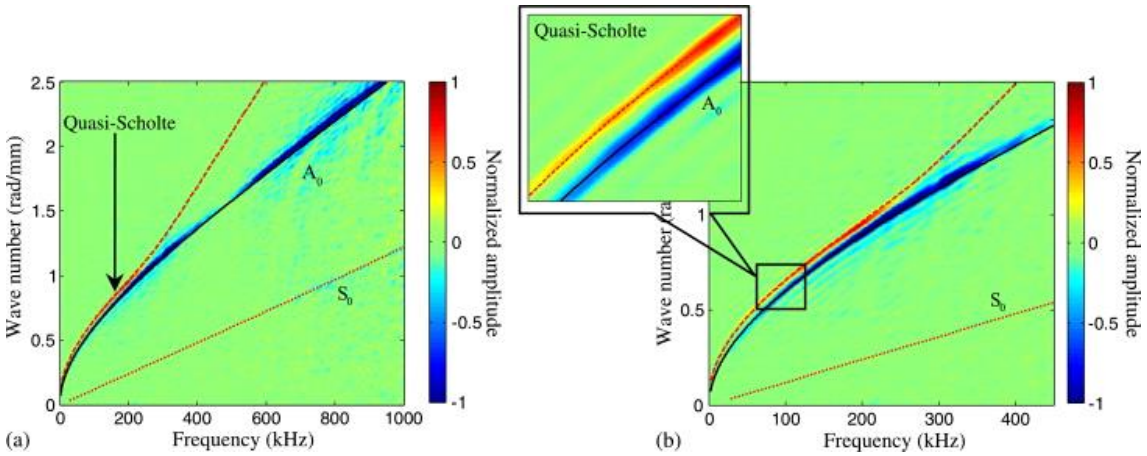

Figure 2.46. The difference obtained by subtracting the free plate spectrum from the immersed plate spectrum [62].

It is concluded that the analysis manifests the presence of guided waves and quasi-Scholte waves in plates partially immersed in water. Study shows that below 300 kHz quasi-Scholte wave dominates. Also, it is found that water influence on the wave propagation is directly related to the length of the water path to the dry path in this study. The sensing system the method can be potentially used for water level detection in a steel container.

CHAPTER 3

GUIDED WAVE PROPAGATION MODEL

3.1. Equation of Motion

Derivation of characteristic equation starts with the equation of motion for an isotropic cubic element in Cartesian coordinates system (x_1, x_2, x_3). The well-known Navier's Equation of Motion is given as in Eqn (3.1) :

$$\begin{aligned} \frac{\partial \sigma_{11}}{\partial x_1} + \frac{\partial \sigma_{12}}{\partial x_2} + \frac{\partial \sigma_{13}}{\partial x_3} &= \rho \frac{\partial^2 u_1}{\partial t^2} \\ \frac{\partial \sigma_{21}}{\partial x_1} + \frac{\partial \sigma_{22}}{\partial x_2} + \frac{\partial \sigma_{23}}{\partial x_3} &= \rho \frac{\partial^2 u_2}{\partial t^2} \\ \frac{\partial \sigma_{31}}{\partial x_1} + \frac{\partial \sigma_{32}}{\partial x_2} + \frac{\partial \sigma_{33}}{\partial x_3} &= \rho \frac{\partial^2 u_3}{\partial t^2} \end{aligned} \tag{3.1}$$

where u_1, u_2 and u_3 are the displacement, ρ is the density of three-dimensional element, t is the time and $\sigma_{11}, \sigma_{22}, \sigma_{33}$ etc. representing the stress field on the faces of this element. In these stress terms, first lower indices are represented normal to plane surface and second indices are showed the directions (x_1, x_2, x_3) respectively.

The stress components are also related by displacements introducing the stress-strain relation for considering isotropic medium be like;

$$\sigma_{ij} = \lambda \varepsilon_{kk} \delta_{ij} + 2\mu \varepsilon_{ij} \tag{3.2}$$

where μ and λ are the Lame parameters for isotropic material. δ_{ij} Representing the Kronecker delta operator with subscript i and j numbering with (1, 2 and 3) corresponding to each direction. For an isotropic elastic material, the equation (3.3) should be satisfied with using the condition in equation (3.4). In this expression displacement tensor is defined as;

$$\varepsilon_{ij} = \frac{1}{2}(u_{i,j} + u_{j,i}) \tag{3.3}$$

$$\delta_{ij} = \begin{Bmatrix} 1 & i = j \\ 0 & i \neq j \end{Bmatrix} \quad , \qquad \varepsilon_{kk} = \varepsilon_{11} + \varepsilon_{22} + \varepsilon_{33} \tag{3.4}$$

where, ε_{kk} represents total change in volume (dilatation) of this element. Substituting Eqn (3.3) and Eqn (3.4) into Eqn (3.2) stress components yields;

$$\begin{gathered} \sigma_{11} = \lambda\varepsilon_{kk}\delta_{ij} + 2\mu\varepsilon_{11}\,, \quad \sigma_{22} = \lambda\varepsilon_{kk}\delta_{ij} + 2\mu\varepsilon_{ij}, \\ \sigma_{33} = \lambda\varepsilon_{kk}\delta_{ij} + 2\mu\varepsilon_{33} \\ \sigma_{12} = 2\mu\varepsilon_{12}, \qquad \sigma_{23} = 2\mu\varepsilon_{23}\,, \qquad \sigma_{13} = 2\mu\varepsilon_{13} \end{gathered} \tag{3.5}$$

The strain-displacement relation can also be respectively written in tensor form and explicitly as;

$$\begin{gathered} \varepsilon_{11} = \frac{\partial_{u1}}{\partial_{x1}}, \qquad \varepsilon_{22} = \frac{\partial_{u2}}{\partial_{x2}}\,, \qquad \varepsilon_{33} = \frac{\partial_{u3}}{\partial_{x3}} \\ \varepsilon_{12} = \frac{\partial_{u1}}{\partial_{x2}} + \frac{\partial_{u2}}{\partial_{x1}}, \qquad \varepsilon_{23} = \frac{\partial_{u2}}{\partial_{x3}} + \frac{\partial_{u3}}{\partial_{x2}}\,, \quad \varepsilon_{13} = \frac{\partial_{u1}}{\partial_{x3}} + \frac{\partial_{u3}}{\partial_{x1}} \end{gathered} \tag{3.6}$$

Substituting the strain-displacement relation in Eqn (3.6) and stress-displacement relation in Eqn (3.5) into the equation of motion, following equations are found:

$$\begin{gathered} (\lambda+\mu)\frac{\partial}{\partial x_1}\left(\frac{\partial u_1}{\partial x_1} + \frac{\partial u_2}{\partial x_2} + \frac{\partial u_3}{\partial x_3}\right) + \mu\nabla^2\partial u_1 = \rho\frac{\partial^2 u_1}{\partial t^2} \\ (\lambda+\mu)\frac{\partial}{\partial x_2}\left(\frac{\partial u_1}{\partial x_1} + \frac{\partial u_2}{\partial x_2} + \frac{\partial u_3}{\partial x_3}\right) + \mu\nabla^2\partial u_2 = \rho\frac{\partial^2 u_2}{\partial t^2} \\ (\lambda+\mu)\frac{\partial}{\partial x_3}\left(\frac{\partial u_1}{\partial x_1} + \frac{\partial u_2}{\partial x_2} + \frac{\partial u_3}{\partial x_3}\right) + \mu\nabla^2\partial u_3 = \rho\frac{\partial^2 u_3}{\partial t^2} \end{gathered} \tag{3.7}$$

Then, Navier's differential equations of motion may be expressed in the vector form as in Eqn (3.8);

$$(\lambda+\mu)\nabla\nabla.\mathbf{u} + \mu\nabla^2\mathbf{u} = \rho\frac{\partial^2\mathbf{u}}{\partial t^2} \tag{3.8}$$

In this expression, ∇ represents the gradient operator ($\widehat{x_1}\frac{\partial}{\partial x_1}, \widehat{x_2}\frac{\partial}{\partial x_2}, \widehat{x_3}\frac{\partial}{\partial x_3}$) and ∇^2 represents the Laplace operator ($\frac{\partial^2}{\partial {x_1}^2} + \frac{\partial^2}{\partial {x_2}^2} + \frac{\partial^2}{\partial {x_3}^2}$). In gradient operator ($\widehat{...}$) symbol represents the vectoral operator for each (x_1, x_2, x_3) directions respectively.

This equation cannot be integrated directly, therefore a form of solutions are needed to be applied on it. Readers may refer to Lowe [33] for detailed explanation of approach and assumptions. It can be explained briefly that there are two solutions, one for "longitudinal" waves and the other for "shear" waves ("bulk waves"). Particle motion in longitudinal waves is completely in the propagation direction and wave motion include only volume change (dilation). Moreover, particle movement in the shear waves are normal to the propagation direction and the movement consists of the rotation of the medium without changing the volume. This approach needs to be presenting the solutions in vector form with Helmholtz method.

3.1.1. Helmholtz Decomposition Method

Helmholtz Decomposition method splits the deformation vector into two parts namely, a scalar potential and a vector potential. These functions are defining dilatational and rotational displacements in a medium respectively. Decomposition is defined as:

$$\mathbf{u} = \nabla\varphi + \nabla \times \psi \tag{3.9}$$

$$\nabla . \psi = \mathbf{0} \tag{3.10}$$

In this representation, displacement fields consist of sum of the gradient of the scalar potential ϕ and curl of the vector potential ψ which correspond to longitudinal and shear waves respectively. Substituting this definition in to Eq. (0.9) yields:

$$(\lambda + \mu)\nabla\big(\nabla . (\nabla\varphi + \nabla \times \psi)\big) + \mu\nabla^2(\nabla\varphi + \nabla \times \psi) = \rho\frac{\partial^2}{\partial t^2}(\nabla\varphi + \nabla \times \psi) \tag{3.11}$$

where , ($\nabla . (\nabla \times \psi) = 0$) and ($\nabla . \nabla\varphi = 0$) must be satisfied individually.

By applying mathematical manipulations and rearranging, the equation may be separated by in terms of scalar and vector function;

$$\nabla\left[(\lambda+\mu)\nabla^2\varphi-\ \rho\frac{\partial^2\varphi}{\partial t^2}\right]+\nabla\times\left[\mu\nabla^2-\rho\frac{\partial^2\psi}{\partial t^2}\right]=0 \tag{3.12}$$

When Helmholtz decomposition is put in the equation of motion, it gives the longitudinal wave motion and shear wave motion as two wave equations (linear, hyperbolic second order partial differential equation):

$$\nabla^2\varphi=\frac{1}{{C_l}^2}\frac{\partial^2\varphi}{\partial t^2} \tag{3.13}$$

$$\nabla^2\psi=\frac{1}{{C_s}^2}\frac{\partial^2\psi}{\partial t^2} \tag{3.14}$$

Where C_l is representing the longitudinal (pressure) P-wave which particle movements parallel to these propagating wave directions and C_s is representing the shear (transverse) S-wave which particle movements perpendicular to direction of the wave propagation. This wave motion leads to rotation motion without causing any changes in volume.

3.1.2. Bulk Velocities of Longitudinal and Shear Waves

This generalized uncoupled wave equation is solved by substituting harmonic wave expression for both functions.

$$\varphi=A_{(L)}e^{i(k.x-\omega t)} \tag{3.15}$$

$$\psi=A_{(S)}e^{i(k.x-\omega t)} \tag{3.16}$$

These general exponential terms are used for describing harmonic wave behavior in medium with time. In these expression, x denotes as three displacement directions,$A(L)$ $A(S)$ are representing the longitudinal and shear wave amplitudes, k is

wavenumber vectors and w is the angular frequency of propagating waves. The wavenumber vector is used for describing propagating wave speed and wavelength with the use of these relations;

$$Wavelength = \frac{2\pi}{k} \text{ and } Phase\ velocity\ (c_{ph}) = \frac{w}{k} \tag{3.17}$$

Substituting these harmonic wave expressions in uncoupled wave equations gives bulk longitudinal and shear wave velocities in terms of mechanical properties of material are obtained as:

$$C_l = \sqrt{\frac{\lambda + 2\mu}{\rho}} = \alpha \quad \text{and} \quad C_s = \sqrt{\frac{\mu}{\rho}} = \beta \tag{3.18}$$

These solutions show that there are two different types of waves that can propagate in isotropic unbounded medium with the constant velocity which is determined by directly using mechanical properties of medium. These Lame parameters μ and λ can be given as;

$$\mu = \frac{E}{2(1+v)} \quad \text{and} \quad \lambda = \frac{Ev}{(1+v)(1-2v)} \tag{3.19}$$

where, E and v are representing Young's modulus and Poisson's ration of the material respectively.

3.2. Guided Waves in Multilayered Media

Previous section bulk wave propagations are considered in unbounded isotropic medium. However, wave propagation is scattering at structure boundaries in terms of reflection and refraction in between parallel surfaces. Therefore, the development of model should be considered with boundaries. First, displacements of longitudinal and shear waves are given after using Helmholtz decomposition:

$$u_{(L)} = \nabla\varphi = \begin{Bmatrix} k_1 \\ k_2 \\ 0 \end{Bmatrix} A_{(L)} e^{i(k.x-\omega t)} \tag{3.20}$$

$$u_{(S)} = \nabla x\psi = \begin{Bmatrix} k_1 \\ -k_2 \\ 0 \end{Bmatrix} A_{(S)} e^{i(k.x-\omega t)} \tag{3.21}$$

Generally, in multi-layered plate models, it is assumed that the wave lengths are considerably smaller than the width of the plate and wave fields, and therefore a plane strain analysis can be applied. The coordinate system can then be reduced in the direction defined by the propagation direction of the waves and the normal of the plate. As can be seen in Figure (3.1), the plane is showed by x_1 parallel to the plate and x_2 normal to the plate. As a result of plane strain assumption, there is no variation of any quantity in the x_3 direction. The interface waves are modeled following with longitudinal (L) and shear (S) partial waves with their directions (+) or (-) defined with respect to positive x_2 direction as seen in Figure (3.1).

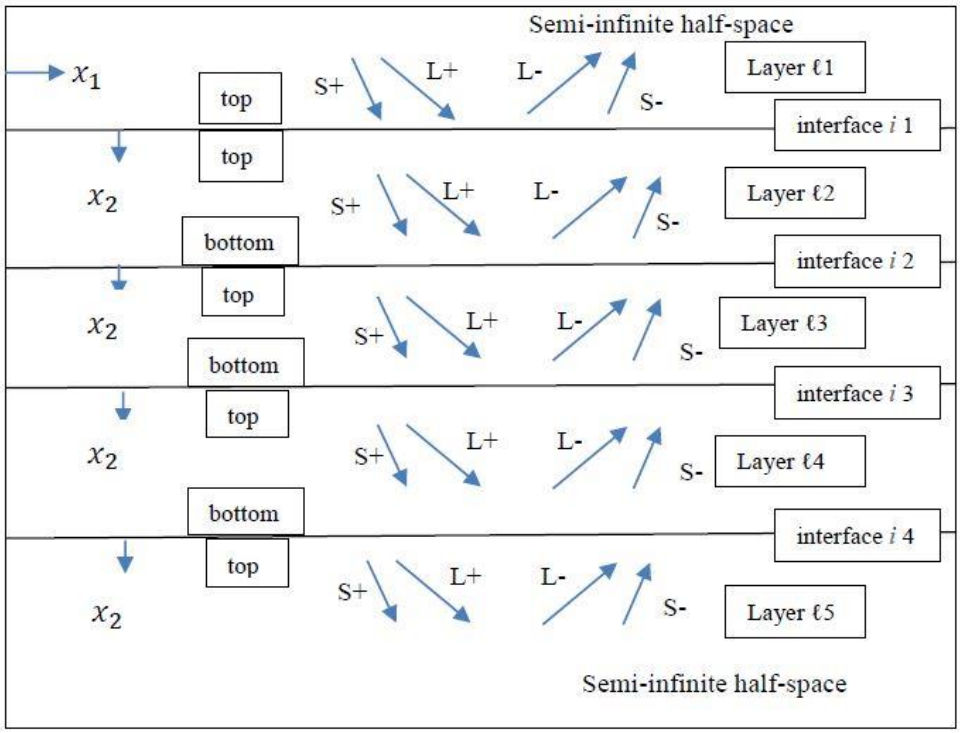

Figure 3.1. Multi-layered plate model.

The exact solution of these equations is made by assuming the harmonic wave $e^{i(kx1-\omega t)}$ type solution for each potential. Where k and ω are wave number and angular frequency respectively. $i=\sqrt{-1}$ and x_1 is representing direction of wave propagation. In consequence of Snell's law, the interaction of waves must share the same frequency and spatial characteristics at each interface in longitudinal direction. Therefore, all field equations for each layer have same factor,F given as:

$$F = e^{i(k_1.x_1-\omega t)} \tag{3.22}$$

Normal component of k_2 can be described by using wave vector and wave speeds of material:

$$k_{2(L^{\pm})} = \pm(\omega^2/\alpha^2 - k_1^2)^{1/2} \tag{3.23}$$

$$k_{2(S^{\pm})} = \pm(\omega^2/\beta^2 - k_1^2)^{1/2} \tag{3.24}$$

Therefore, displacements and stresses in a layer can be evaluated by means of the amplitudes of the bulk waves. Moreover, longitudinal and shear bulk waves can be separated to model the multilayered system.

For longitudinal bulk waves:

$$\begin{gathered}
u_1 = k_1 A_{(L^{\pm})} F e^{\pm i(\omega^2/\alpha^2 - k_1^2)^{1/2} x_2} \\
u_2 = \pm(\omega^2/\alpha^2 - k_1^2)^{1/2} A_{(L^{\pm})} F e^{\pm i(\omega^2/\alpha^2 - k_1^2)^{1/2} x_2} \\
\sigma_{11} = (\omega^2 - 2\beta^2\,\omega^2/\alpha^2 + 2\beta^2 k_1^2) i\rho A_{(L^{\pm})} F e^{\pm i(\omega^2/\alpha^2 - k_1^2)^{1/2} x_2} \\
\sigma_{22} = (\omega^2 - 2\beta^2 k_1^2) i\rho A_{(L^{\pm})} F e^{\pm i(\omega^2/\alpha^2 - k_1^2)^{1/2} x_2} \\
\sigma_{33} = (1 - 2\,\beta^2/\alpha^2) i\omega^2 \rho A_{(L^{\pm})} F e^{\pm i(\omega^2/\alpha^2 - k_1^2)^{1/2} x_2} \\
\sigma_{12} = \pm 2\beta^2 k_1 (\omega^2/\alpha^2 - k_1^2)^{1/2}\, i\rho A_{(L^{\pm})} F e^{\pm i(\omega^2/\alpha^2 - k_1^2)^{1/2} x_2} \\
\sigma_{13} = \sigma_{23} = 0
\end{gathered} \tag{3.25}$$

For shear bulk waves:

$$
\begin{aligned}
u_1 &= \pm(\omega^2/\beta^2 - k_1^2)^{1/2} A_{(S_-^+)} F e^{\pm i(\omega^2/\,\beta^2 - k_1^2)^{1/2} x_2} \\
u_2 &= -k_1 A_{(S_-^+)} F e^{\pm i(\omega^2/\,\beta^2 - k_1^2)^{1/2} x_2} \\
\sigma_{11} &= \pm 2\beta^2 k_1 (\omega^2/\,\beta^2 - k_1^2)^{1/2}\, i\rho A_{(S_-^+)} F e^{\pm i(\omega^2/\,\beta^2 - k_1^2)^{1/2} x_2} \\
\sigma_{22} &= -\sigma_{11} \\
\sigma_{12} &= (\omega^2 - 2\beta^2 k_1^2) i\rho A_{(S_-^+)} F e^{\pm i(\omega^2/\,\beta^2 - k_1^2)^{1/2} x_2} \\
\sigma_{33} &= \sigma_{13} = \sigma_{23} = 0
\end{aligned}
\tag{3.26}
$$

The displacements and stresses in any position of the layer can be found by taking the four wave components in the layer. Modifications can be made on the obtained equations to simplify modeling as it is given:

$$
\begin{aligned}
C_\alpha &= (\omega^2/\alpha^2 - k_1^2)^{1/2},\ C_\beta = (\omega^2/\beta^2 - k_1^2)^{1/2} \\
g_\alpha &= e^{\pm i(\omega^2/\alpha^2 - k_1^2)^{1/2} x_2},\ g_\beta = e^{\pm i(\omega^2/\beta^2 - k_1^2)^{1/2} x_2} \\
B &= \omega^2 - 2\beta^2 k_1^2
\end{aligned}
\tag{3.27}
$$

3.2.1. The Global Matrix Method

The Global Matrix Method is used for obtaining the dispersion characteristics of the multilayer structure to develop matrix representation for the boundary conditions of the layer system. Matrix representation includes the stress and displacement variables that are necessary for satisfying the boundary conditions. Therefore, aim is to assemble a robust single linear matrix equation which represents the complete system. The global matrix consists of $4(\mathrm{n}-1)$ equations, where n is the total number of layers perfectly bonded together with each interface. The solution is done by solving all of the equations for the whole matrix simultaneously. Interfaces are dependent in each other, because the equations at an interface are influenced by the arrival of waves from the neighboring interfaces.

As mentioned before, the interface waves are modeled following with longitudinal (L) and shear (S) partial waves with their directions (+) or (-) defined with respect to positive x_2 direction as seen in Figure (3.1). At the semi-infinite half spaces of liquids, only the waves directed away from the interface, and in the intermediate layers all four partial waves are considered. In case of vacuum half spaces, there are no waves at the half spaces. Some assumptions should be made in the model.

Traction-free condition is used for at the inner and outer interfaces of the entire system. Each layer is homogeneous and isotropic and infinitely long in the longitudinal direction (x_1). Traction-free conditions are given below:

$$\begin{Bmatrix}\sigma_{22}\\ \sigma_{12}\end{Bmatrix}_{\substack{Free\\ Surface}} = 0 \tag{3.28}$$

Also, there are interfacial continuity conditions between any two layers which are the continuity of displacement components and the normal and shear components of the stress. This can be shown as:

$$\begin{Bmatrix}u_1\\ u_2\\ \sigma_{22}\\ \sigma_{12}\end{Bmatrix}_{\substack{Layer=i\\ Interface=i+1}} = \begin{Bmatrix}u_1\\ u_2\\ \sigma_{22}\\ \sigma_{12}\end{Bmatrix}_{\substack{Layer=i+1\\ Interface=i+1}} \tag{3.29}$$

All things considered, matrix expression of any position in a plate layer can be presented as:

$$\begin{Bmatrix}u_1\\ u_2\\ \sigma_{22}\\ \sigma_{12}\end{Bmatrix} = [M]\begin{Bmatrix}A_{(L+)}\\ A_{(L-)}\\ A_{(S+)}\\ A_{(S-)}\end{Bmatrix} e^{i(kx_1-\omega t)} \tag{3.30}$$

where [M] is called a layer matrix.

Layer matrix $[M_{ij}]$ describes the layer as the ith layer at the jth interface. In order to define layer matrix at a free surface, new matrix can be written because it has only stress quantities. Layer matrix for free surfaces can be expressed as:

$$[M_{11}]\{A_1\} = 0$$
$$\left[M_{n(n+1)}\right]\{A_n\} = 0 \tag{3.31}$$

The boundary condition at the interface between arbitrary layers can be shown as:

$$\left[M_{i(i+1)}\right]\{A_i\} = \left[M_{(i+1)(i+1)}\right]\{A_{i+1}\} \tag{3.32}$$

For example, layers are shown as Figure (3.1), the displacements and stresses at the second interface is function of the amplitudes of the waves at the top of the third layer. But, it can be also described as function of the amplitudes of the waves at the bottom of the second layer. Moreover, (33) can be written in a single matrix by taking all terms to the left-hand side of the equation.

$$\left[M_{i(i+1)}\right]\left[-M_{(i+1)(i+1)}\right]\begin{Bmatrix}\{A_i\}\\ \{A_{i+1}\}\end{Bmatrix} = 0 \tag{3.33}$$

By using free surface and continuity conditions, the global matrix can be assembled for a system that includes all boundary conditions. The system equation has to be zero because of no energy added to the system.

$$[G]\{A\} = 0 \tag{3.34}$$

For instance, a global matrix of 4-Layer system can be build up as a following structure:

$$G = \begin{bmatrix} [N_{11}] & 0 & 0 & 0 \\ [M_{12}] & [M_{22}] & 0 & 0 \\ 0 & [M_{23}] & [M_{33}] & 0 \\ 0 & 0 & [M_{34}] & [M_{44}] \\ 0 & 0 & 0 & [N_{45}] \end{bmatrix} \tag{3.35}$$

This approach is used for three-layer axially symmetric longitudinal wave case and boundary conditions are applied for interface 1 as between layer 1 and layer 2:

$$\begin{aligned} u_n^y &\quad \cdots \quad n = component, y = layer\ number \\ \sigma_n^y &\quad \cdots \quad n = component, y = layer\ number \\ M_n^y &\quad \cdots \quad n = component, y = layer\ number \end{aligned} \tag{3.36}$$

$$u_1^1 = u_2^2 \qquad M_{12}^1 + M_{14}^1 = M_{11}^2 + M_{12}^2 + M_{13}^2 + M_{14}^2]_{interface_1} \tag{3.37}$$

$$u_1^1 = u_2^2 \qquad M_{22}^1 + M_{24}^1 = M_{21}^2 + M_{22}^2 + M_{23}^2 + M_{24}^2]_{interface_1} \tag{3.38}$$

$$\sigma_{22}^1 = \sigma_{22}^2 \qquad M_{32}^1 + M_{34}^1 = M_{31}^2 + M_{32}^2 + M_{33}^2 + M_{34}^2]_{interface_1} \tag{3.39}$$

$$\sigma_{12}^1 = \sigma_{12}^2 \qquad M_{42}^1 + M_{44}^1 = M_{41}^2 + M_{42}^2 + M_{43}^2 + M_{44}^2]_{interface_1} \tag{3.40}$$

Same procedure is applied for interface 2 as between layer 2 and layer 3:

$$u_1^2 = u_2^3 \qquad M_{11}^2 + M_{12}^2 + M_{14}^2 + M_{13}^2 = M_{11}^3 + M_{13}^3 +]_{interface_2} \tag{3.41}$$

$$u_1^2 = u_2^3 \qquad M_{21}^2 + M_{22}^2 + M_{23}^2 + M_{24}^2 = M_{21}^3 + M_{23}^3]_{interface_2} \tag{3.42}$$

$$\sigma_{22}^2 = \sigma_{22}^3 \qquad M_{31}^2 + M_{32}^2 + M_{33}^2 + M_{34}^2 = M_{31}^3 + M_{33}^3]_{interface_2} \tag{3.43}$$

$$\sigma_{12}^2 = \sigma_{12}^3 \qquad M_{41}^2 + M_{42}^2 + M_{43}^2 + M_{44}^2 = M_{41}^3 + M_{43}^3]_{interface_2} \tag{3.44}$$

Then putting all terms into a single matrix, the global matrix ‘G’ for the three-layer system is generated as shown below:

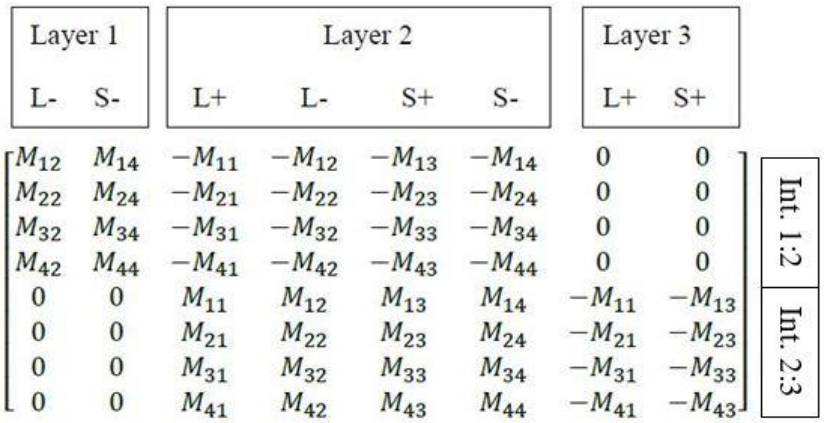

Figure 3.2. Global matrix of three layered system.

To implement the global matrix into the Matlab, the presented scheme can be used.

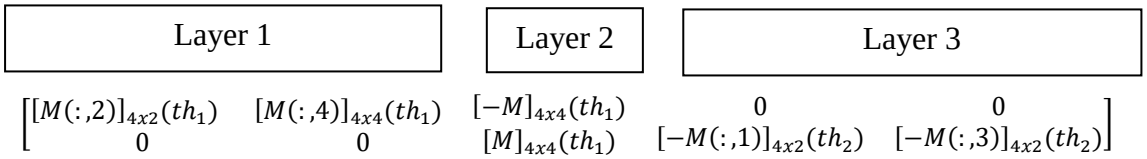

$$\begin{bmatrix} [M(:,2)]_{4x2}(th_1) & [M(:,4)]_{4x4}(th_1) & [-M]_{4x4}(th_1) & 0 & 0 \\ 0 & 0 & [M]_{4x4}(th_1) & [-M(:,1)]_{4x2}(th_2) & [-M(:,3)]_{4x2}(th_2) \end{bmatrix}$$

Figure 3.3. Global matrix scheme used in Matlab.

After obtaining the global matrix, modal solution for the multilayer system is ready to evaluate by solving for the frequency and wave number values which are the roots of the characteristic equation. This solution provides us to understand how ultrasonic guided waves propagate in an elastic planar structure.

If it is summarized what was done so far:

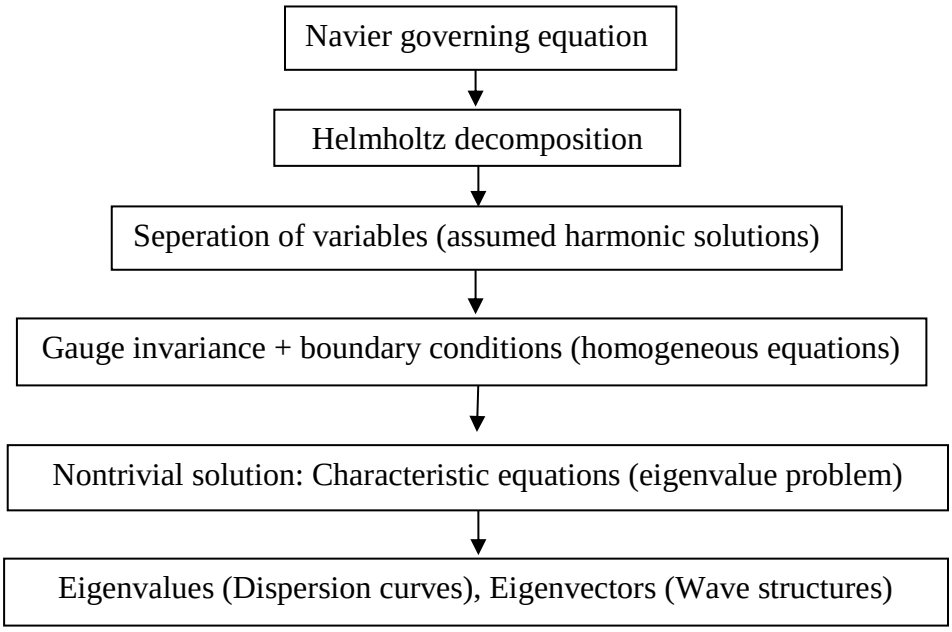

Figure 3.4. Summarized flowchart of analysis.

3.2.1.1. Liquid Boundaries

Treatment for fluid materials should be done for Scholte Waves which includes liquid interfaces. In this treatment, ideal liquids are used that do not support shear. For this reason, tangential stresses must be zero at the interface, while tangential stresses are transmitted along the interface as they are for solid-solid boundaries. In addition, there will be no restrictions on locally tangential relocations, since the two materials are free to slip over each other. However, the normal displacement and compressional stress of the boundary must still be continuous throughout the interface.

$$u_2]_{solid\ at\ interface} = u_2]_{liquid\ at\ interface}$$
$$\sigma_{22}]_{solid\ at\ interface} = \sigma_{22}{}_{liquid\ at\ interface}$$
$$\sigma_{12}]_{solid\ at\ interface} = \sigma_{12}]_{liquid\ at\ interface}$$

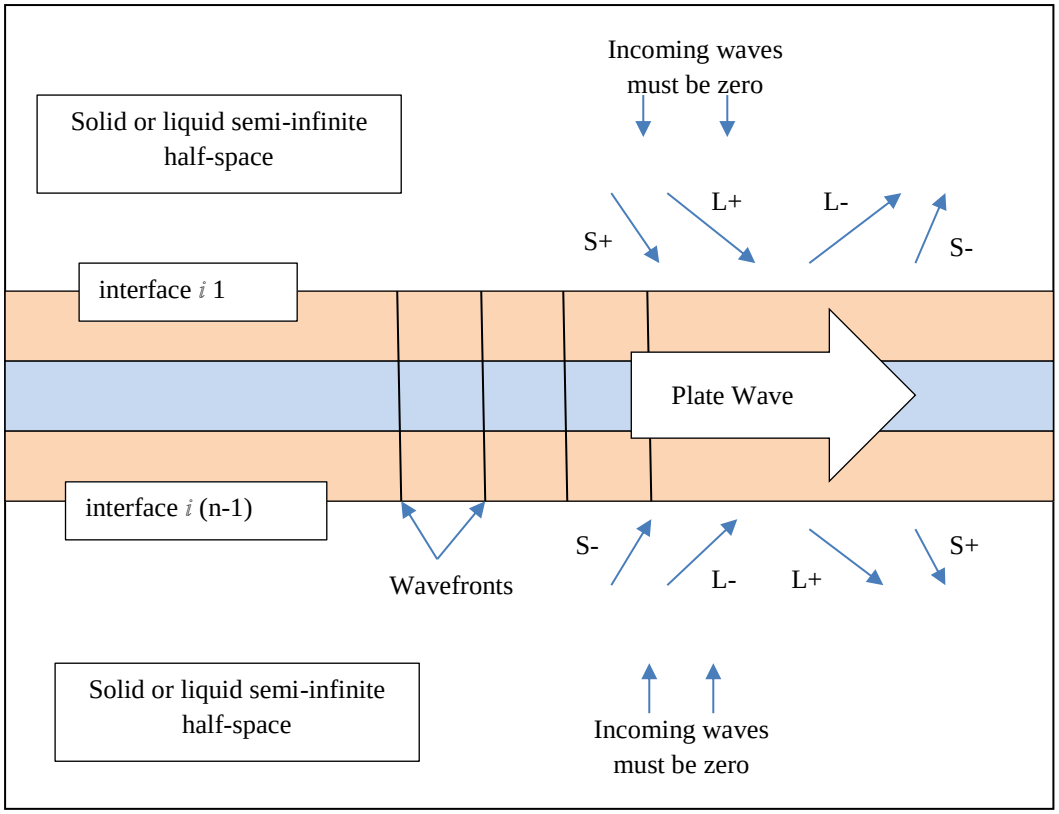

Figure 3.5. Boundary conditions of plate in solid or liquid-semi infinite half-space.

At the semi-infinite half spaces of liquids, only the waves directed away from the interface, and in the intermediate layers all four partial waves are considered. Following the convention of Lowe, continuity of the displacements in x_1 and x_2, and continuity of the stresses in 11 and 12 directions at the interfaces are considered.

$$\begin{Bmatrix} u_1 \\ u_2 \\ \sigma_{22} \\ \sigma_{12} \end{Bmatrix} = \begin{bmatrix} k_1 g_\alpha & \frac{k_1}{g_\alpha} & C_\beta g_\beta & \frac{-C_\beta}{g_\beta} \\ C_\alpha g_\alpha & \frac{-C_\alpha}{g_\alpha} & -k_1 g_\beta & \frac{k_1}{-g_\beta} \\ \mathrm{i}\rho B g_\alpha & \frac{\mathrm{i}\rho B}{g_\alpha} & -2\mathrm{i}\rho k_1 \beta^2 C_\beta g_\beta & \frac{2\mathrm{i}\rho k_1 \beta^2 C_\beta g_\beta}{g_\beta} \\ -2\mathrm{i}\rho k_1 \beta^2 C_\alpha g_\alpha & \frac{-2\mathrm{i}\rho k_1 \beta^2 C_\alpha}{g_\alpha} & \mathrm{i}\rho B g_\beta & \frac{\mathrm{i}\rho B}{g_\beta} \end{bmatrix} \cdot \begin{Bmatrix} A_{(L+)} \\ A_{(L-)} \\ A_{(S+)} \\ A_{(S-)} \end{Bmatrix}$$

The solution of the system for the phase velocity can be done by numerically solving for the phase velocities which make the determinant zero. The results of the model

and numerical calculations were verified with the free demo version of DISPERSE software with titanium and motor oil for pure and quasi-Scholte modes and with multiple results from literature and the results are given in Chapter 4.

3.2.2. Numerical Approach

The inputs of the layered system are material properties and layer thicknesses, there are two unknown variables: frequency w, and wavenumber, k. Solution of characteristic function depends on these two variables. Analytical solution is very difficult and not available, therefore numerical searching methods have to be used. For generating dispersion curves, one of the variables (k or w) is kept constant while the other variable is being searched for the solution.

In general, roots of the characteristic equations are real, imaginary or complex. If there are no attenuating terms in system, the roots are purely real as like presented case. If roots are purely imaginary which is critically damped, those correspond to the non-propagating, or evanescent wave modes. If a propagating wave is attenuating with distance from the source, roots of the system will be complex.

3.2.3. Numerical Results

In the analysis, purely elastic media and waves are considered. Bisection method is used with incremental starting values to obtain the dispersion curve roots.

The phase velocity dispersion curves show the velocity of the harmonic wave cycles in the direction of propagation along the structure; they provide useful information about wave speeds of single tones and of wavelengths of the modes. As an application example, relatively long lengths of plates can be inspected for corrosion and cracking from a single probe position. This saves a great deal of time and money compared to using more standard point-by-point normal beam inspection. Moreover, composites which are made of laminated structure can be inspected without removing layers or coatings by controlling guide wave modes and frequencies.

CHAPTER 4

EXPERIMENTAL STUDY

4.1. Set-up

4.1.1. Dipstick Method

The experimental setup used is designed to utilize the quasi-Scholte mode on a plate immersed in a liquid and to measure group velocity. Figure (4.1) shows the picture of experimental set up.

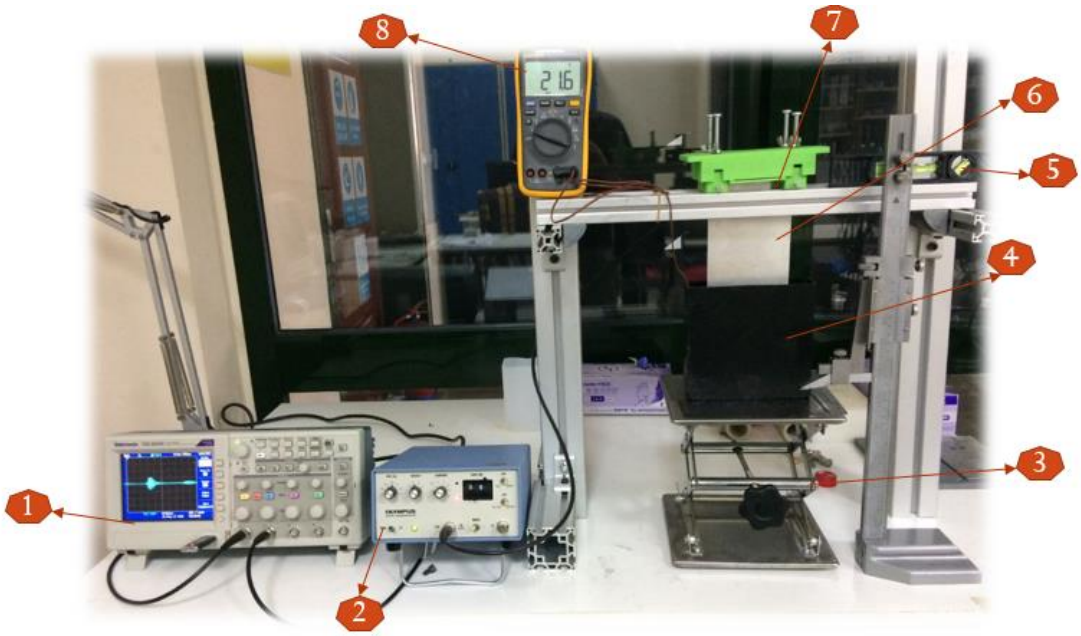

Figure 4.1. Experimental setup for dipstick method.

1- Tektronix TD 2024C oscilloscope

2- Olympus 5072PR

3- Table with variable height

4- Fluid container

5- Spirit level device

6- Dipstick

7- Adjunct device

8- Fluke digital multimeter

0.5 MHz contact shear transducer (Olympus V151) was used to excite quasi-Scholte wave mode in Aluminum plate. The Pulser-Receiver is connected to the shear transducer and to the oscilloscope. 1mm thick aluminum plate is fixed perpendicular to the transducer surface by using an adjunct device.

The center of aluminum plate is attached perpendicular to the transducer surface. It is assembled to the transducer at 90 degrees of axis to produce out-of-plane movements uniformly throughout the thickness of the plate. In this way, A0 mode is created in a reliable manner on the free plate, which are converted to Scholte waves upon entry to fluid region.

As a shear couplant, wax was used between the transducer and aluminum plate. Shear wave could propagate better with help of a couplant. Honey and glycerol are also used as couplant, but optimum image is obtained when the wax is used.

Liquid container placed under aluminum plate which is attached on transducer by using adjunct device. The adjunct apparatus was designed and then manufactured by using a 3D printer. Liquid container could move up and down on by an adjustable table. By altering the height of the table, the plate can be properly immersed in the liquid at various depths. It is important that the plate is immersed in the liquid in a perpendicular manner.

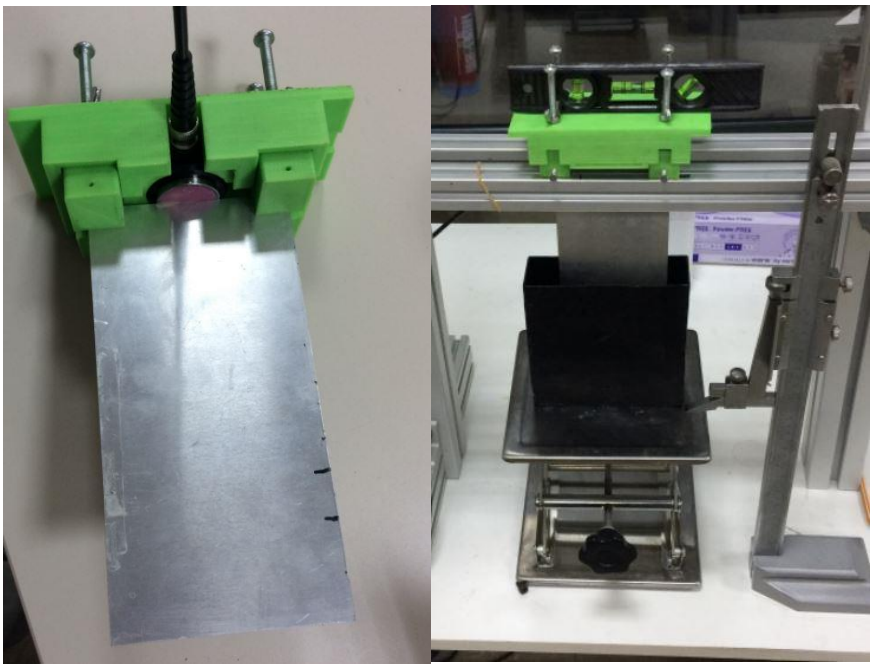

Figure 4.2. Aluminum plate and sensor connections.

Temperature of liquid was controlled by using Fluke digital multimeter test device. The temperature was recorded simultaneously while the measurements were taken.

Electrical pulses formed by from Olympus 5072PR Pulser/Receiver are used for generating and then sensing ultrasonic waves. Desired properties such as energy, damping and gain are set on this device. Tektonix TD 2024C scope was used to monitor the signals. Finally, MATLAB® software code, which is published by Tektronix, was used to process the signals.

4.1.2. Tensile Test

As mentioned earlier, with using equation (3.18) and (3.19) longitudinal (c_l) and shear (c_s) velocity of the material can be calculated by using its Young's modulus (E), poisson ratio (v) and density (ρ). These material properties need to be calculated for the velocity results to be clear. As we were unable to find the exact values of Young's modulus for the metal waveguide, we used tensile testing to obtain it. Samples were prepared for tensile test machine, Shimadzu AG-IC in IZTECH Mechanical Engineering laboratory. Dimensions of samples are 25 mm x 150 mm x 1 mm. The stress-strain plot obtained by the tensile test is given in Figure (4.3). Young's modulus of aluminum along the direction of interest was found to be $62\ GPa$. Poisson's ration of Al plate is taken from literature. Then, the density was calculated as$2695\ kg/m^3$.

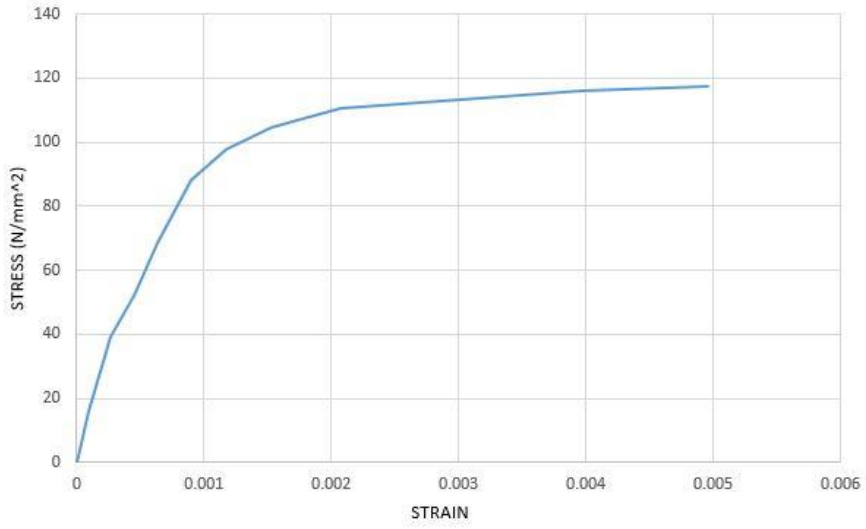

Figure 4.3. Stress-Strain diagram for 1mm aluminum plate.

Table 1. Mechanical properties of Al plate.

Material Type	Max Stress at Entire Area (N/mm^2)	Young's Modulus (GPa)	Poisson's Ratio (v)
Aluminum	117.4	62.74	0.34

Aluminum plate used for measurements was 200mm long and 100mm wide and it had $\rho = 2695\ kg/m^3, c_l = 5950\ m/s, c_s = 2930\ m/s$. The calculated material property values were also compared with the results of velocity measurements, which are used fundamental guided wave modes.

4.1.3. Test Cell Method

Bulk wave properties of the fluid must be known to validate of quasi-Scholte mode. An ultrasonic test cell method was used to find the bulk wave velocities as done in University of Nottingham [60].

PVC pipes suitable for the contact diameter of the transducers are used as test cell. Two pipes were attached together and two test cells were obtained at different lengths. 0,5 MHz Longitudinal transducers (Olympus A101S) were attached opposite sides of test cell as shown in Figure (4.4). Based on the distance between transducers and time of flight, velocity of bulk waves could be calculated.

Figure 4.4. Ultrasonic test cells at different distances.

4.2. Signal Processing

In many applications of nondestructive materials evaluation, precise determination of the time content of a signal is very important. In most cases, exact location or timing of the signals has to be found to evaluate group velocity by directly analysis of the time-domain signals. Threshold crossing, also known as “first break” determination, is often the method of choice [63]. In this method, the threshold voltage value is used to determine the arrival time of a given waveform. Each of these methods is prone to errors due to changes in the shape of the pulses as they traverse a sample. On the other hand, since the frequency values are high, short sweeping intervals are employed. A small shift in the selected point in the time domain has found to lead to a large error. Also, other methods for determination of relative time locations make use of frequency domain information as well. Deconvolution by spectral division and complex spectral analysis are two examples. The topic of this thesis is the use of phase information for finding time shifts.

In order to determine the group velocity, firstly Fourier transform is applied to the Hanning-windowed signal and then the zero-phase slope method is applied on obtained fast Fourier transform. When the window is aligned with the group arrival time of a frequency component of the signal, the phase slope of the frequency component will show zero tendency. Thus, the group arrival time is calculated by scanning the time domain signal on a window and evaluating the phase slope for each frequency, when the frequency group arrival coincides with the window center, zero phase slope point is obtained. This can be described by using the shift property of Fourier Transform [34]:

$$
\begin{aligned}
F\big(f(t)\big) &= \int_{-T}^{+T} f(t)e^{-i\omega t}dt = F(\omega) \\
F\left(f\big(t-t_{shift}\big)\right) &= \int_{-T}^{+T} f\big(t-t_{shift}\big)e^{-i\omega t}dt = \\
&\int_{-T}^{+T} f\big(t-t_{shift}\big)e^{-i\omega\left(t-t_{shift}\right)}e^{-i\omega t_{shift}}d\left(t-t_{shift}\right) \\
&= e^{-i\omega t_{shift}}F(\omega)
\end{aligned}
\tag{4.1}
$$

Fourier transform of the displacement signal of a traveling wave can be modeled as:

$$F(u(x,t)) = F(\omega)e^{-ikx}e^{-i\emptyset_0} \tag{4.2}$$

when the time origin of the signal is shifted to the right by a delay t_{shift} the shifting property of the Fourier Transform leads to the expression below

$$F(u(x,t))_{t_{shift}} = F(\omega)e^{-ikx}e^{-i\emptyset_0}e^{-i\omega t_{shift}} \tag{4.3}$$

Expression is also shown as:

$$F(u(x,t))_{t_{shift}} = F_1 e^{-i\emptyset_e} \tag{4.4}$$

where F_1 is a constant and Φ_e is the overall phase angle whose components are:

$$\emptyset_e = -i(kx + \emptyset_0 + \omega t_{shift}) \tag{4.5}$$

therefore, the phase slope can be evaluated from

$$\frac{d\emptyset_e}{d\omega} = \frac{dk}{d\omega}x - t_{shift} \tag{4.6}$$

and putting group velocity expression $c_g = \frac{d\omega}{dk}$ into the equation

$$\frac{d\emptyset_e}{d\omega} = -\frac{x}{c_g} - t_{shift} \tag{4.7}$$

The only condition except the $x \neq 0$ that fulfills the equation in zero phase slope is the following expression

$$\frac{d\emptyset_e}{d\omega} = 0 = -\frac{x}{c_g} - t_{shift} = -T_g - t_{shift} \tag{4.8}$$

and time shift can be determined as

$$T_g = -t_{shift} \tag{4.9}$$

then using equation 4.9, the group velocity of the signal can be found as

$$c_g = \frac{x_2 - x_1}{\frac{d\emptyset_{e_1}}{d\omega} - \frac{d\emptyset_{e_2}}{d\omega}} T_g = -t_{shift} \tag{4.10}$$

Signal processing can be summarized as follows. Firstly, reflected signals from two different lengths in the material are observed. Then Fast Fourier Transform was applied to the time series to find the spectra of Hanning windowed signals. Then, the phase was unwrapped and the phase slope was calculated as shown in Figure (4.5). It was seen that if signal is a clear, the performance of the method will be very good.

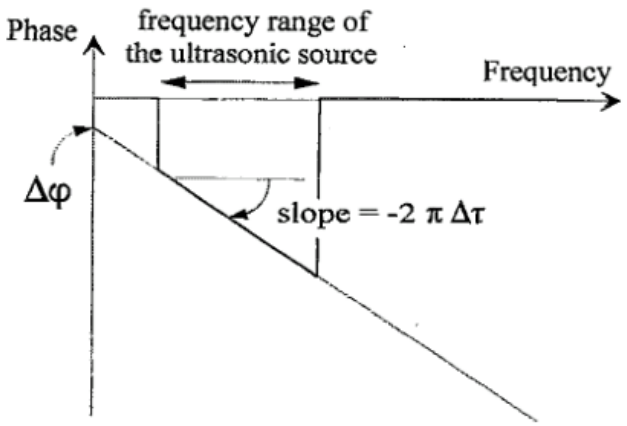

Figure 4.5. Phase Slope Plotting. [2]

As mentioned before, the signal is sent and received by Pulser/Receiver and stored by the oscilloscope. Then the data is transferred to a PC for processing. Processing is expressed by following steps:

- Signals are received at two different distances, at two different dipping depths. Figure (4.6) shows transmitted and the received signal of %8 ethanol-alcohol mixtures at room temperatures.

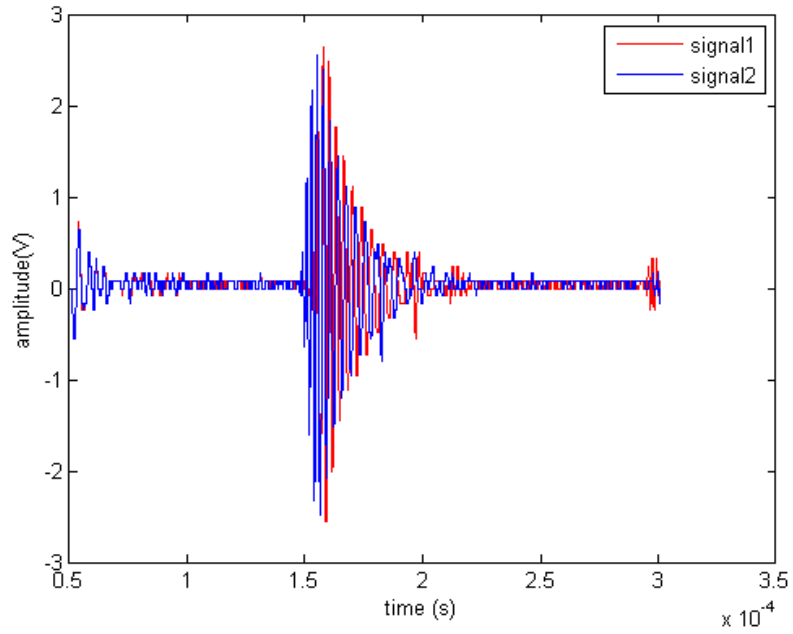

Figure 4.6. Two received signals from different immersed depths.

- 0.5 MHz shear transducer was used to create quasi-Scholte wave modes. FFT of two received signals are shown in Figure (4.7). FFT method converts the time domain signal to frequency domain. Peak points of FFT of the signal represent the natural frequency of the shear transducer.

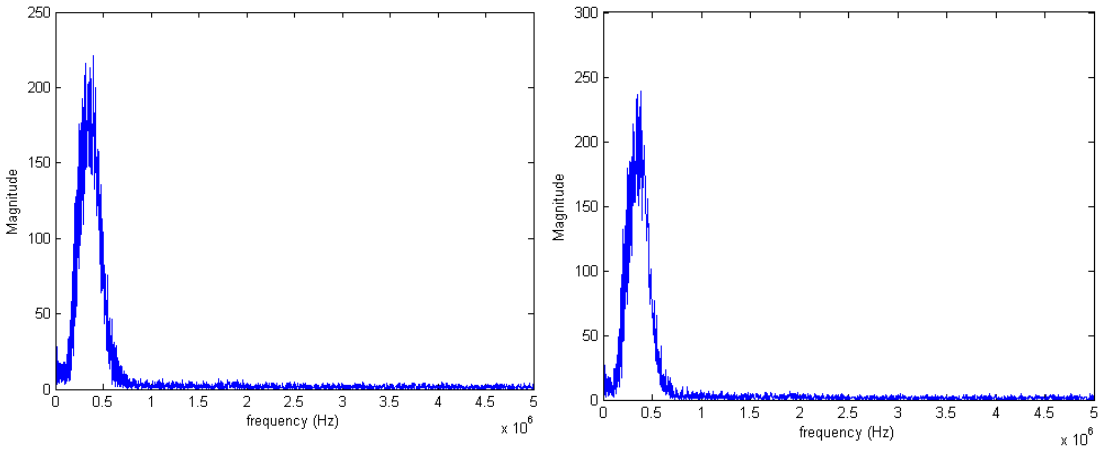

Figure 4.7. FFT of two received signals.

- The following expression is applied to the frequency domain signal, then phase can be found.

$$phase = \frac{imaginary\ part\ of\ signal}{real\ part\ of\ signal}$$

- The phase is evaluated at different frequencies and the slope is found as seen in the Figure (4.8). In order to calculate the time of flight, ±0.15 MHz range of 0.5 MHz transducer was taken into consideration. A line-fit was used on phase slope curve. This line is drawn with reference to 0.65 MHz-0.35 MHz which is the operating range of the transducer.

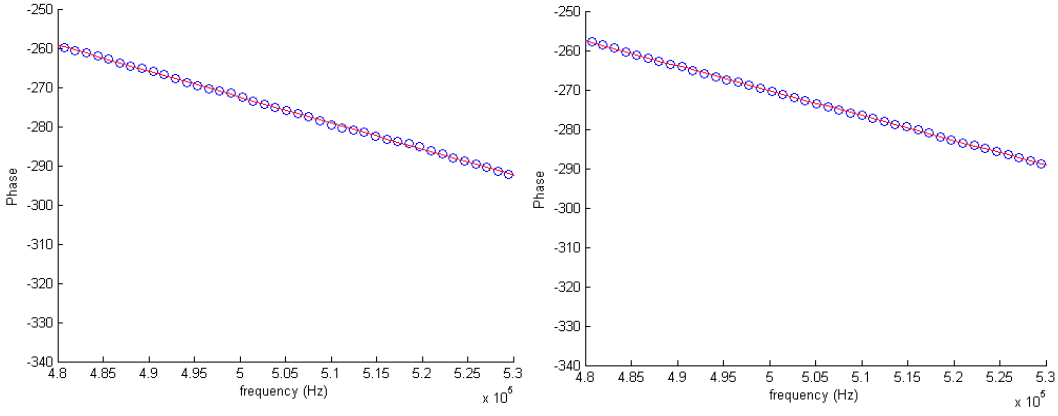

Figure 4.8. Phase slopes of the signals.

- Phases which are shown in Figure (4.8) are put into the Equation (4.10), then phase slope is found. The most important part is that, transmitted and received signals should not contain high levels of noise.

4.3. Measurements

4.3.1. Experimental Results of Longitudinal Bulk Wave

Mixtures of ethanol-water with concentration ratios %5-8-10-15-20-25-30 are prepared according to their mass ratio. Firstly, water and ethanol were mixed in a container by using electromagnetic stirrer. Density measurements of the mixtures in room temperature done with an alcohol-meter are shown at Table (2).

Table 2. Measured density of ethanol-water mixtures at room temperature.

Percent %	%5	%8	%10	%15	%20	%25	%30
Density (kg/m3)	988.30	938.50	980.39	973.5	966.5	958	950.8

Longitudinal wave velocities of mixtures in room temperature were measured by using two PVC pipes, which have different wave paths (72.8 mm).

Results are calculated and shown at Table (3) according to time of flight and distance difference.

Table 3. Longitudinal wave velocities of mixtures in room temperature.

Percent %	%5	%8	%10	%15	%20	%25	%30
Velocity (m/s)	1530.5	1554.2	1567.1	1596.5	1615	1620.8	1595.1

Measured Longitudinal Bulk wave velocities at different temperatures graphed as Figure (4.9).

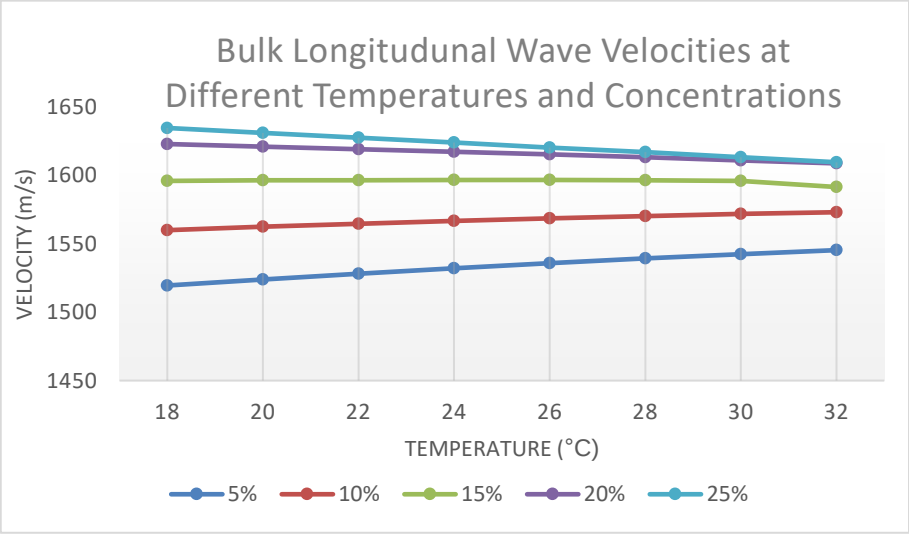

Figure 4.9. Bulk and longitudinal wave velocities at different temperatures and concentrations.

4.3.2. Scholte Wave Experimental Results

An aluminum plate of 1 mm in thickness, whose mechanical properties was determined, immersed in the fluid. Results were taken at two different depths. These two depths are significant to monitoring the wanted wave type. For example, if aluminum plate immersed in too deep, the received wave cannot be monitored clearly. On the contrary, if the immersed depth is too shallow, different modes of signals can be monitored and selecting the right one is difficult, such as the leaky Rayleigh wave.

At the beginning, a comparison was made with the results of DISPERSE program to prove the validity of in-house code. Dispersion curves were plotted for 1 mm thick titanium plate immersed in motor oil. The result from the DISPERSE program is shown in Figure (4.10).

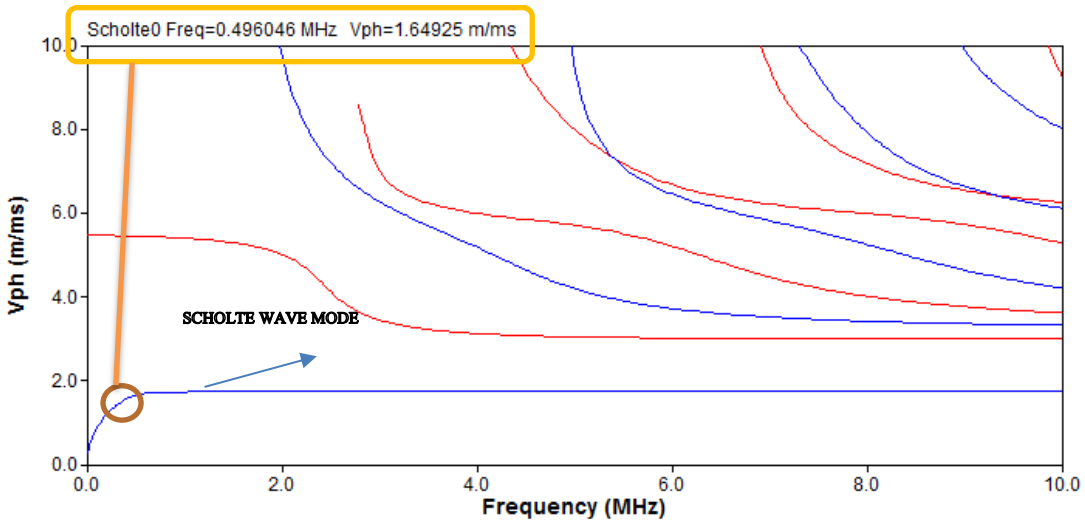

Figure 4.10. Phase velocity dispersion curves of 1mm Titanium plate immersed in motor oil.

The properties of titanium and engine oil are taken from the software so that the code can be compared properly with the program. The result from code for Scholte wave phase velocity of 1mm thick titanium plate immersed in motor oil is shown in Figure (4.11).

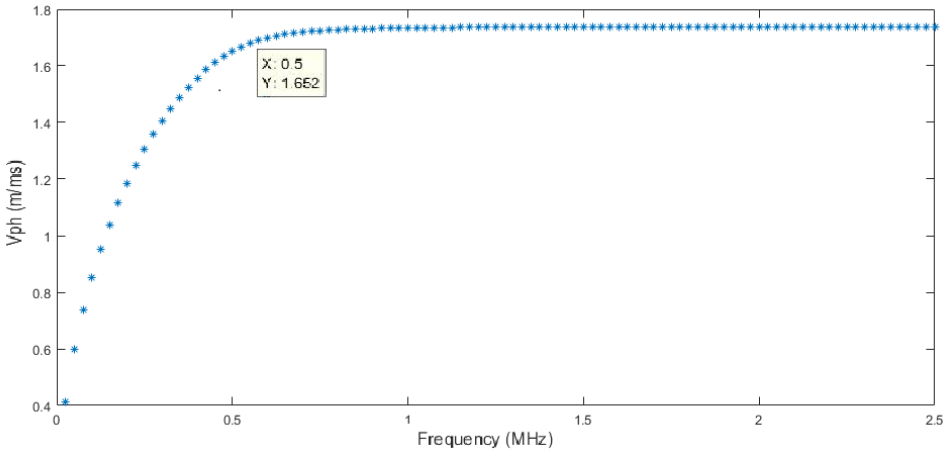

Figure 4.11. Phase velocity Scholte wave dispersion curves of 1mm Titanium plate immersed in motor oil.

At 22 °C ethanol distilled water mixtures of different concentrations were calculated by using Scholte code in MATLAB solver.The resulting phase velocity frequency curves are superimposed on the same Figure (4.12) up to 10 MHz range.In order to obtain those curves, acoustic and material properties are determined from the test cell methods and the tensile test results. These properties are summerized in Table (1) and Table (3).

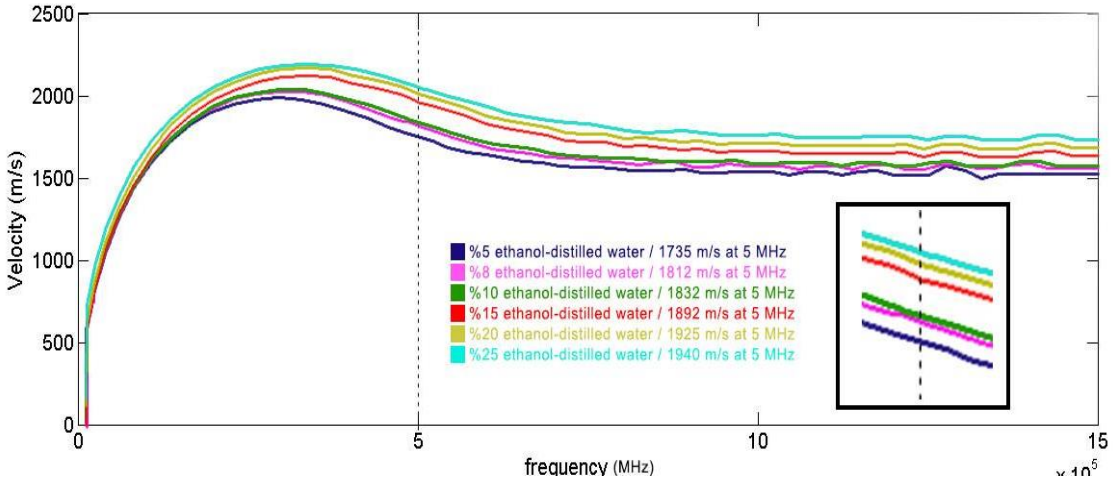

Figure 4.12. Calculated Scholte wave velocities of ethanol water mixtures at different concentrations.

Table 4 shows the comparison in between measured and the theoretical velocity calculations of different ethanol water concentrations.

Table 4. QS Wave velocity at 22°C

Ethanol-Water concentration of mass	Measured Velocity (m/s)	Theoretical Velocity (m/s)	Relative Error (%)	Distance Between Immersion Depths (mm)
%5	1729.4	1735	0.322	9,5
%8	1812.3	1812	0.016	15,6
%10	1827.4	1832	0.272	9,6
%15	1897.5	1892	0.563	19
%20	1920.9	1925	0.212	9,4
%25	1938.1	1940	0.103	9,5

4.4. Error Consideration

Various errors and problem are encountered in both bulk wave experiments and quasi Scholte mode experiments and are explained below.

Test cells are used in bulk wave experiments. Nevertheless, the results differ from literature and coded results by % 6.1. Besides that, reflections from the surface of the test cells are commonly observed. These reflections made it harder to specify the longitudinal bulk wave. To solve this problem, various containers were used, but lastly distance between two transducers is decided to be shortened and PVC pipes were used. Reflections also occurred in PVC pipes, but these reflections could be identified easily because they have very low amplitudes. Another advantage of the PVC pipe is that the transducers on the test cells are usually hard to center. In PVC pipes, the transducers are automatically centered. Also, the diameter of PVC pipes was chosen to perfectly fit to transducers and be in direct contact to the liquid. Reflections and misleading factors made it impossible to take measurements in other containers. Disadvantage of these pipes is that, the liquid must be heated to be able to take measurements at different temperatures. The liquid is heated in another vessel and then poured in test cell and its temperature is observed until it reaches the desired temperature. This caused a waste of time and errors in measurements because the temperature was not stable during the test. Although a small amount of

solution could have been used for measurements. Measurement results are found to have an uncertainty of %1 interval using PVC tubes.

Better results are obtained with the setup for Scholte wave measurements. At first, the depth of the container for liquid is observed to be too shallow. The immersed plate caused the wave to reflect off of container wall and then the container is enlarged and widened.

Another parameter is the coupler material that is needed to be put between the transducer and the plate for transmission. Honey, glycerol and wax are used for this purpose. Wax is determined to show the best performance.

It is essential for measurements that the immersed plate to be perpendicular to the liquid, also the transducer to be perpendicular to the plate. A spirit level device is used for every experiment.

Immersion levels in the system are measured with a vertical caliper of 0.05 mm resolution. For the calculations of the reflected wave measurements to be correct, the wave needs to be recorded with good resolution and noise must be in acceptable levels. Otherwise FFTs and phase slopes do not provide a solution.

When the same distance between two immersed depths are used in different concentrations, waveforms are not properly obtained. Waves are observed in oscilloscope and datas of correct waveforms with correct distance between immersed depths are used. Distances in experiments are not standard for this reason.

Function generator cannot be used in measurements with a single transducer. For this reason, natural frequency of the transducer is used a transmit and receive process is performed. This made hard to process the reflected wave.

Modes similar to leaky-Rayleigh waves are also observed when immersion depth is short. Required mode is observed by changing the immersed depth. But when the immersed depth is too high, phase slopes of obtained forms are observed to be too noisy to be specified. Measurements are taken between 50 mm – 100 mm immersed depths for this reason.

CHAPTER 5

CONCLUSION

The objective of this thesis is using Scholte wave to characterize the fluid. For this purpose, wave propagation has been generated observed, and the mathematical modelling has been examined.

Guided wave and bulk wave phenomena have been discussed. Comparison of dipstick and test cell method has been investigated. Using quasi Scholte mode and calculating time of flight by dipstick method to reach a result was intended.

At first mathematical infrastructure of wave propagation was examined, modelled analytically and solved by global matrix method. An in-house developed code which is called as Scholte code was used to solve these equations where MATLAB is employed as a coding language. The results were then compared with commercial DISPERSE program and their compablity is observed.

Modelled waves are examined experimentally. Longitudinal bulk velocities of the liquid are needed to find quasi Scholte wave results through this code. Two setups were constructed for both measurements. One is the test cell setup for measuring longitudinal bulk wave velocity, second is the dipstick setup for measuring quasi Scholte wave velocity.

Test cells were prepared with Plexiglas and iron material to measure longitudinal bulk wave velocities. Through-transmission, pulse and echo methods were used. PVC pipes are used as container because this makes errors more acceptable. In quasi-Scholte mode measurements, an aluminum plate is used as a waveguide. It is immersed in different depths in various specimens. Also, measurements are taken with unimmersed plate and different Lamb wave modes are observed. This validates that the system is working. Various container types are used and it is seen that when the noise is less on the walls of the container, the measurement results are better. The errors observed are thoroughly explained in chapter 4 in error section.

Differences between the velocities obtained from Scholte wave velocities and the in-house codes are shown in table 5 in relative error section. These results are obtained with determining the errors one by one and making optimizations.

It is concluded that, QS wave mode can be used for liquid characterization in closed containers. This method can be improved with designing a more stable and more practical sensor. This is because the sensor used for this study is constructed with different parts and this makes the measurements vulnerable to human error. Further improvement of this method can lead to a more user friendly and precise measurements in industrial and everyday usage.

REFERENCES

[1] Rose, J. L. (2014). Ultrasonic guided waves in solid media. Ultrasonic Guided Waves in Solid Media (pp. 1–512). https://doi.org/10.1017/CBO9781107273610

[2] J. Krautkramer and H. Krautkramer. Ultrasonic Testing of Materials. 3rd edition. Springer-Verlag, 1983.

[3] A C Kak, M Slaney, Principles of computerized tomographic imaging, IEEE Press, New York (1988)

[4] J. Blitz. Electrical and Magnetic Methods of Nondestructive Testing. Chapman and Hall, 1997.

[5] Cho, Y. (2000). Estimation of ultrasonic guided wave mode conversion in a plate with thickness variation. IEEE transactions on ultrasonics, ferroelectrics, and frequency control, 47(3), 591-603.

[6] Source: ‘’ http://www.olympus-ims.com/en/ndt-tutorials/flaw-detection/wave-propagation ‘’

[7] Rayleigh, Lord. (1885). On waves propagated along the plane surface of an elastic solid. Proceedings of the London Mathematical Society, s1-17(1), 4–11. https://doi.org/10.1112/plms/s1-17.1.4

[8] Jia, Junbo. Modern Earthquake Engineering: Offshore and Land-based Structures. Springer, 2016.

[9] Lamb, H. (1917). On Waves in an Elastic Plate. Proceedings of the Royal Society A: Mathematical, Physical and Engineering Sciences, 93(648), 114–128.

[10] Cho, Younho, et al. "A study on the guided wave mode conversion using self-calibrating technique." Roma 2000 15th World Conference on Non-Destructive Testing. 2000.

[11] Alleman, G., Pelt, M. M. J. M., & Groves, R. M. (2014, October). Air-coupled ultrasound for damage detection in CFRP using Lamb waves and ultrasonic verification. In Proc. ICAST2014: 25nd International Conference on Adaptive Structures and Technologies, The Hague.

[12] Holnicki-Szulc, J., & Soares, C. M. (Eds.). (2013). Advances in smart technologies in structural engineering (Vol. 1). Springer Science & Business Media.

[13] Torkamani, S., Roy, S., Barkey, M. E., Sazonov, E., Burkett, S., & Kotru, S. (2014). A novel damage index for damage identification using guided waves with application in laminated composites. Smart Materials and Structures, 23(9), 095015.

[14] Zerwer, A., Polak, M. A., & Santamarina, J. C. (2003). Rayleigh wave propagation for the detection of near surface discontinuities: Finite element modeling. Journal of nondestructive evaluation, 22(2), 39-52.

[15] Cegla, F.B., Ultrasonic Waveguide Sensors for Fluid Characterisation and Remote Sensing, in Department of Mechanical Engineering. 2006, Imperial College London: London, UK. p. 248.

[16] McLean, J., & Degertekin, F. L. (2004). Directional scholte wave generation and detection using interdigital capacitive micromachined ultrasonic transducers. IEEE Transactions on Ultrasonics, Ferroelectrics, and Frequency Control, 51(6), 756–764. https://doi.org/10.1109/TUFFC.2004.1304274

[17] Stoneley, R. (1924). Elastic Waves at the Surface of Separation of Two Solids. Proceedings of the Royal Society A: Mathematical, Physical and Engineering Sciences, 106(738), 416–428. https://doi.org/10.1098/rspa.1924.0079

[18] Ávila-Carrera, R., Spurlin, J. H., & Valle-Molina, C. (2011). Simulating elastic wave propagation in boreholes: Fundamentals of seismic response and quantitative interpretation of well log data. Geofísica internacional, 50(1), 57-76.

[19] Scholte, J. G. (1942). On the Stoneley wave equation. Proceedings of the Koninklijke Nederlandse Akademie van Wetenschappen, 45(part 1), 20-25.

[20] Glorieux, C., Van de Rostyne, K., Nelson, K., Gao, W., Lauriks, W., & Thoen, J. (2001). On the character of acoustic waves at the interface between hard and soft solids and liquids. The Journal of the Acoustical Society of America, 110(3), 1299-1306.

[21] Padilla, F., de Billy, M., & Quentin, G. (1999). Theoretical and experimental studies of surface waves on solid–fluid interfaces when the value of the fluid sound velocity is located between the shear and the longitudinal ones in the solid. The Journal of the Acoustical Society of America, 106(2), 666-673.

[22] Every, A.G., R.E. Vines, and J.P. Wolfe, Line-focus probe excitation of Scholte acousticwaves at the liquid-loaded surfaces of periodic structures. Physical Review B, 1999.60(16): p. 11755-11760.

[23] Glorieux, C., Van de Rostyne, K., Goossens, J., Shkerdin, G., Lauriks, W., & Nelson, K. A. (2006). Shear properties of glycerol by interface wave laser ultrasonics. Journal of applied physics, 99(1), 013511

[24] Desmet, C., Gusev, V., Lauriks, W., Glorieux, C., & Thoen, J. (1996). Laser-induced thermoelastic excitation of Scholte waves. Applied physics letters, 68(21), 2939-2941.

[25] Moiseyenko, R. P., Declercq, N. F., & Laude, V. (2013). Guided wave propagation along the surface of a one-dimensional solid–fluid phononic crystal. Journal of Physics D: Applied Physics, 46(36), 365305.

[26] Fan, Z. (2010). Applications of guided wave propagation on waveguides with irregular cross-section (Doctoral dissertation, Imperial College London).

[27] Cho, Y., & Rose, J. L. (1996). A boundary element solution for a mode conversion study on the edge reflection of Lamb waves. The Journal of the Acoustical Society of America, 99(4), 2097-2109.

[28] Cawley, P., & Adams, R. D. (1979). The location of defects in structures from measurements of natural frequencies. The Journal of Strain Analysis for Engineering Design, 14(2), 49-57.

[29] Liu, G. R., & Achenbach, J. D. (1995). Strip element method to analyze wave scattering by cracks in anisotropic laminated plates. TRANSACTIONS-AMERICAN SOCIETY OF MECHANICAL ENGINEERS JOURNAL OF APPLIED MECHANICS, 62, 607-607.

[30] Thomson, W. T. (1950). Transmission of elastic waves through a stratified solid medium. Journal of Applied Physics, 21(2), 89–93. https://doi.org/10.1063/1.1699629

[31] Haskell, N. A. (1990). The Dispersion of Surface Waves on Multilayered Media, Vol. 30. American Geophysical Union, Washington, DC.

[32] L. Knopoff. A matrix method for elastic wave problems. Bulletin of the Seismological Society of America, 54:431–438, 1964.

[33] Lowe, M. J. (1995). Matrix techniques for modeling ultrasonic waves in multilayered media. IEEE transactions on ultrasonics, ferroelectrics, and frequency control, 42(4), 525-542.

[34] Cegla, F. B. (2006). Ultrasonic waveguide sensors for fluid characterisation and remote sensing (Doctoral dissertation, Imperial College London).

[35] Kossoff, G. (1966). The effects of backing and matching on the performance of piezoelectric ceramic transducers. IEEE Transactions on sonics and ultrasonics, 13(1), 20-30.

[36] Sen, S. N. (1990). Acoustics, waves and oscillations. New Age International.

[37] Prüll, C. (2007). Generation and detection of Lamb waves for the characterization of plastic deformation (Doctoral dissertation, Georgia Institute of Technology).

[38] Challis, R. E., Harrison, J. A., Holmes, A. K., & Cocker, R. P. (1991). A wide bandwidth spectrometer for rapid ultrasonic absorption measurements in liquids. The Journal of the Acoustical Society of America, 90(2), 730-740.

[39] Cegla, F. B., Cawley, P., & Lowe, M. J. S. (2005). Material property measurement using the quasi-Scholte mode—A waveguide sensor. The Journal of the Acoustical Society of America, 117(3), 1098-1107.

[40] Holnicki-Szulc, J., & Soares, C. M. (Eds.). (2013). Advances in smart technologies in structural engineering (Vol. 1). Springer Science & Business Media.

[41] Cawley, P., & Alleyne, D. (1996). The use of Lamb waves for the long range inspection of large structures. Ultrasonics, 34(2-5), 287-290.

[42] Lowe, M. J., Alleyne, D. N., & Cawley, P. (1998). Defect detection in pipes using guided waves. Ultrasonics, 36(1-5), 147-154.

[43] Zhu, W., Rose, J. L., Barshinger, J. N., & Agarwala, V. S. (1998). Ultrasonic guided wave NDT for hidden corrosion detection. Journal of Research in Nondestructive Evaluation, 10(4), 205-225.

[44] Chang, Z., & Mal, A. (1999). Scattering of Lamb waves from a rivet hole with edge cracks. Mechanics of materials, 31(3), 197-204.

[45] Wang, C. S., Wu, F., & Chang, F. K. (2001). Structural health monitoring from fiber-reinforced composites to steel-reinforced concrete. Smart materials and Structures, 10(3), 548.

[46] Wang, L., & Yuan, F. G. (2007). Active damage localization technique based on energy propagation of Lamb waves. Smart Structures and Systems, 3(2), 201-217.

[47] Viktorov, I. A. (2014). Rayleigh and lamb waves: physical theory and applications (ultrasonic technology). Springer.

[48] Doyle, P. A., & Scala, C. M. (1978). Crack depth measurement by ultrasonics: a review. Ultrasonics, 16(4), 164-170.

[49] Angel, Y. C., & Achenbach, J. D. (1984). Reflection and transmission of obliquely incident Rayleigh waves by a surface-breaking crack. The Journal of the Acoustical Society of America, 75(2), 313-319.

[50] Dong, R., & Adler, L. (1984). Measurements of reflection and transmission coefficients of Rayleigh waves from cracks. The Journal of the Acoustical Society of America, 76(6), 1761-1763.

[51] Rose, J. L., Ditri, J. J., Pilarski, A., Rajana, K., & Carr, F. (1994). A guided wave inspection technique for nuclear steam generator tubing. NDT & E International, 27(6), 307-310.

[52] Rose, J. L., & Mudge, P. J. (2002, June). Flexural mode focusing in pipe. In 8th European Conference on Non-Destructive Testing, Barcelona, Spain (pp. 17-21).

[53] Thompson, R. B., Alers, G. A., & Tennison, M. A. (1972, October). Application of direct electromagnetic Lamb wave generation to gas pipeline inspection. In 1972 Ultrasonics Symposium (pp. 91-94). IEEE.

[54] Van Velsor, J. K., Rose, J. L., & Nestleroth, J. B. (2009). Enhanced Coating Disbond Detection Capabilities in Pipe Using Circumferential Shear Horizontal Guided Waves. Materials Evaluation, 67(10), 1179-1188.

[55] Chimenti, D. E., & Nayfeh, A. H. (1990). Ultrasonic reflection and guided wave propagation in biaxially laminated composite plates. The Journal of the Acoustical Society of America, 87(4), 1409-1415.

[56] Puthillath, P., & Rose, J. L. (2010). Ultrasonic guided wave inspection of a titanium repair patch bonded to an aluminum aircraft skin. International Journal of Adhesion and Adhesives, 30(7), 566-573.

[57] Gao, H., & Rose, J. L. (2009). Ice detection and classification on an aircraft wing with ultrasonic shear horizontal guided waves. IEEE transactions on ultrasonics, ferroelectrics, and frequency control, 56(2), 334-344.

[58] Van Velsor, J. K., Gao, H., & Rose, J. L. (2007). Guided-wave tomographic imaging of defects in pipe using a probabilistic reconstruction algorithm. Insight-Non-Destructive Testing and Condition Monitoring, 49(9), 532-537.

[59] Graff, K. F. (2012). Wave motion in elastic solids. Courier Corporation.

[60] Takiy, A. E., Granja, S. C. G., Higuti, R. T., Kitano, C., Elvira, L., Martinez-Graullera, O. F., & de Espinosa, F. M. (2013, July). Theoretical analysis and experimental validation of the scholte wave propagation in immersed plates for the characterization of viscous fluids. In Ultrasonics Symposium (IUS), 2013 IEEE International (pp. 1614-1617). Ieee.

[61] Wilkie-Chancellier, N., Martinez, L., Serfaty, S., & Griesmar, P. (2009). Lamb wave sensor for viscous fluids characterization. IEEE Sensors Journal, 9(9), 1142–1147. https://doi.org/10.1109/JSEN.2009.2027411

[62] Yu, L., & Tian, Z. (2015). Case study of guided wave propagation in a one-side water-immersed steel plate. Case Studies in Nondestructive Testing and Evaluation, 3, 1-8.

[63] Chang, F. K. (Ed.). (2013). Structural Health Monitoring 2013: A Roadmap to Intelligent Structures: Proceedings of the Ninth International Workshop on Structural Health Monitoring, September 10–12, 2013. DEStech Publications, Inc.